CrossMark

Projected changes of summer monsoon extremes and hydroclimatic regimes over West Africa for the twenty-first century

Ismaïla Diallo[1,2,3] · Filippo Giorgi[2] · Abdoulaye Deme[4] · Moustapha Tall[3] · Laura Mariotti[2] · Amadou T. Gaye[3]

Abstract We use two CORDEX-Africa simulations performed with the regional model RegCM4 to characterize the projected changes in extremes and hydroclimatic regimes associated with the West African Monsoon (WAM). RegCM4 was driven for the period 1970–2100 by the HadGEM2-ES and the MPI-ESM Global Climate Models (GCMs) under the RCP8.5 greenhouse gas concentration pathway. RegCM4 accurately simulates the WAM characteristics in terms of seasonal mean, seasonal cycle, interannual variability and extreme events of rainfall. Overall, both RegCM4 experiments are able to reproduce the large-scale atmospheric circulation for the reference period (i.e. present-day), and in fact show improved performance compared to the driving GCMs in terms of precipitation mean climatology and extreme events, although different shortcomings in the various models are still evident. Precipitation is projected to decrease (increase) over western (eastern) Sahel, although with different spatial detail between RegCM4 and the corresponding driving GCMs. Changes in extreme precipitation events show patterns in line with those of the mean change. The models project different changes in water budget over the Sahel region, where the MPI projects an increased deficit in local moisture supply (E < P) whereas the rest of models project a local surplus (E > P). The E–P change is primarily precipitation driven. The precipitation increases over the eastern and/ or central Sahel are attributed to the increase of moisture convergence due to increased water vapor in the boundary layer air column and surface evaporation. On the other hand, the projected dry conditions over the western Sahel are associated with the strengthening of moisture divergence in the upper level (850–300 hPa) combined to both a southward migration of the African Easterly Jet (AEJ) and a weakening of rising motion between the core of the AEJ and the Tropical Easterly Jet.

Keywords Climate change · CORDEX · RegCM4 · West African summer monsoon climate · Precipitation extreme · Hydrological cycle · Dynamical downscaling

✉ Ismaïla Diallo
ismaila1.diallo@ucad.edu.sn; idiallo@ucla.edu

1   Department of Geography, University of California, Los Angeles (UCLA), 315 Portola Plaza, #1255 (Bunche Hall, UCLA), Los Angeles, CA 90095, USA

2   Earth System Physics Section, The Abdus Salam International Centre for Theoretical Physics (ICTP), 34151 Trieste, Italy

3   Laboratoire de Physique de l'Atmosphère et de l'Océan Siméon Fongang (LPAO-SF), Ecole Supérieure Polytechnique, Université Cheikh Anta Diop (ESP-UCAD), Dakar, Senegal

4   Université Gaston Berger de Saint Louis, Unité de Formation et de Recherche Sciences Appliquées et technologie (UFR-SAT), Ngalléle/Saint Louis, Senegal

1 Introduction

The most prominent tools used to study climate change due to increasing atmospheric concentrations of greenhouse gases (GHG) are coupled Atmosphere/Ocean Global Climate Models (AOGCMs) [Intergovernmental Panel on Climate Change (IPCC), 2007]. While all previous studies based on AOGCM projections agree on a future GHG-induced warming trend in West Africa, no consensus is found about changes in the precipitation and water cycle, and the uncertainties remain large (Druyan 2011). Though AOGCMs can satisfactorily simulate the atmospheric general circulation at the continental scale, they cannot capture

the detailed processes associated with regional and/or local climate variability and changes that are required for regional and national climate change assessments (Giorgi and Mearns 1999; Giorgi et al. 2009; Rummukainen 2010). This is particularly true for heterogeneous regions such as West Africa (WA), where local conditions associated with topography (Diallo et al. 2014; Moufouma-Okia and Jones 2015), vegetation (Nicholson 2013), land-sea distribution and landuse types (Sylla et al. 2013a; Zaroug et al. 2013) have a significant effect on climate. For instance, Cook and Vizy (2006); Xue et al. (2010) and Diallo et al. (2014) pointed out that GCMs simulate poorly the main features responsible for triggering and maintaining the West African Monsoon (WAM) rainfall. In addition, the coarse-resolution climate information is not sufficient to support agricultural applications at the local level (Giorgi et al. 2009; Oettli et al. 2011); Vizy et al. 2013.

Regional Climate Models (RCMs) are often used to dynamically downscale AOGCMs output or global analyses of observations (i.e. reanalysis). They can better describe fine-scale physical processes and greater detail of local land surface and topography (Giorgi and Mearns 1999; Sylla et al. 2013a). Significant efforts have been dedicated to the simulation and the characterization of atmospheric water cycle components worldwide either for the current or the future climate (Music and Caya 2009; Mariotti et al. 2008; Mariotti 2010; Prasanna and Yasunari 2011; Bhaskaran et al. 2012; Alpert et al. 2013; Otieno and Anyah 2013; Siam et al. 2013). Nevertheless, RCM-based studies focusing on the characterization of the atmospheric water cycle over the West African region have been limited (e.g. Van Den Hurk and Van Meijgaard 2010; Sylla et al. 2012). For instance Van Den Hurk and Van Meijgaard (2010) investigated land–atmosphere interactions at climatological time scales using different diagnostic in experiments with the RACMO2.1 RCM, while Sylla et al. (2012) found wetter conditions over the different West African highlands in the middle and late twenty-century from RegCM3 driven with the ECHAM5 output. They associated these wetter conditions to an enhancement of the atmospheric hydrological cycle.

To fill this gap, a number of recent international projects such as the ENSEMBLES-African Monsoon Multidisciplinary Analysis (AMMA) (Van der Linden et Mitchell 2009), the West African Monsoon Modeling and Evaluation (WAMME) (Druyan et al. 2010; Xue et al. 2010) and the ongoing COordinated Regional Climate Downscaling EXperiment (CORDEX; Giorgi et al. 2009) have focused on the application of RCMs over West Africa or the whole African continent. Work from these projects investigated the performance of RCMs in reproducing the key current mean climatology of the region (Hernandez-Diaz et al. 2012; Nikulin et al. 2012; Panitz et al. 2013; Gbobaniyi

et al. 2013; Diallo et al. 2014; Kluste et al. 2016), projected changes in mean seasonal climate and higher order statistics (Laprise et al. 2013; Bouagila and Sushama 2013; Paeth et al. 2011) and processes underlying differences in change signals between RCMs and driving GCMs (Saeed et al. 2013; Mariotti et al. 2014). In particular Paeth et al. (2011) emphasized the large uncertainty still present in RCM projections over the region. Clearly, more detailed analysis is needed to better understand the processes characterizing the simulated changes in the hydrologic cycle over West Africa.

Therefore, in this work we extend the analysis of Mariotti et al. (2014) of two RCM projections over an all-Africa CORDEX domain and undertake a more detailed analysis focusing mainly over the West Africa region. The purpose of the present paper is to understand the dynamical processes associated with the projected changes in mean and extreme precipitation and how these are related to the atmospheric water balance characteristics of different areas in the WAM region. Note that the investigation of structural bias of these simulations and an analysis of the added value of downscaling low-resolution AOGCMs over the present climate (historical runs) are presented in Coppola et al. (2014) and Diallo (2015), respectively. Also, we recall that, the analysis presented here, does not intend to provide comprehensive scenario projection with associated uncertainties, but rather to quantify whether RCMs produce different projections signals than their driving AOGCMs, using a single RCM driven by two different AOGCMs.

The paper is organized as follows: Sect. 2 presents the model configuration; experimental design as well as the method including the satellite and gauge based observational datasets used for validation and comparisons. Results and discussions are presented in Sect. 3, where the seasonal mean, annual cycle and interannual variability of precipitation, the large scale atmospheric circulations as well as the rainfall extreme events are validated, before providing an overview of projected change in mean precipitation extremes, atmospheric water budget and moisture transport. Finally, summary and main conclusions are given in Sect. 4.

2 Model description, simulation design and observation dataset

2.1 Model description and simulation design

In this study we used the Regional Climate Model version 4.2 (hereafter, RegCM4) in the same configuration described in Mariotti et al. (2014). RegCM4, developed at the Abdus Salam International Centre for Theoretical Physics (ICTP) is described by Giorgi et al. (2012), while a full description of RegCM4 simulations for CORDEX-Africa is

Fig. 1 CORDEX African domain and its topography (in meter, m) at 50 km resolution. Squares in **a** indicate the West African regions and in **b** The West African domain (WA) with highlight of the different sub-regions (West Sahel, Sahel; Guinea) and orographic features: GH (Guinea highlands), JP (Jos Plateau), and CM (Cameroun Mountains)
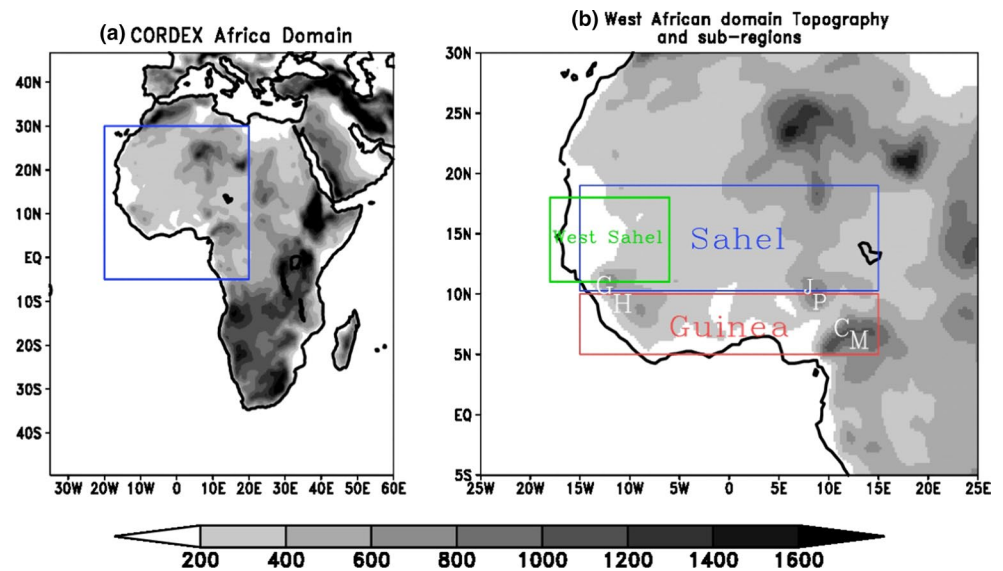
given in Coppola et al. (2014). Earlier version of this model were described and documented by Giorgi et al. (1993a, b), Giorgi and Mearns (1999), Pal and Coauthors (2007). RegCM4 is a compressible primitive equation, sigma vertical coordinate model with dynamics based on the hydrostatic version of the National Centre for Atmospheric Research/Pennsylvania State University's Mesoscale Meteorological Model version 5 (NCAR/PSU's MM5; Grell et al. 1994). The model includes multiple options of physics parameterizations. Therefore based on previous works (e.g. Diallo et al. 2010; Sylla et al. 2013a; Mariotti et al. 2011; Diallo et al. 2015) as well as a series of preliminary experiment tests, the following options are used: a modified radiative package of the NCAR Community Climate Model version 3 (CCM3; Kiehl et al. 1996), the nonlocal vertical diffusion scheme of Holstag et al. (1990) to represent the boundary layer processes, the subgrid explicit moisture (SUBEX) resolvable scale precipitation scheme of Pal et al. (2000) and the scheme of Zeng et al. (1998) to represent fluxes from ocean surfaces. Note that, RegCM4 introduces several improvements over RegCM3 including coupling with one-dimensional lake model, new land surface, planetary boundary layer and air-sea flux schemes, a mixed convection and tropical band option, modifications to the pre-existing radiative and boundary layer schemes and a full upgrade of the model code (Giorgi et al. 2012).

The RegCM4 simulations analyzed here was the object of a first analysis presented in Mariotti et al. (2014) over Africa, which focused on the intra-seasonal characteristics of African monsoon climates. In fact, RegCM4 was integrated over the recommended CORDEX domain for Africa (Giorgi et al. 2009; Jones et al. 2011—see Fig. 1a) with a horizontal grid spacing of 50 km and 18 vertical levels

for the period 1970–2100. In these experiments, Meteorological and 6-h lateral boundary conditions (LBCs) as well as sea surface temperatures (SSTs) necessary to run the model are taken from two different Atmospheric Ocean Global Climate Models (AOGCMs) under historical, i.e. current-climate (reference; RF) and future Representative Concentration Pathways 8.5 (RCP 8.5) emission scenario corresponding to a high greenhouse gas emissions pathway compared to the scenario literature (IPCC 2008). One AOGCM is the Earth system version of the Max-Planck-Institut für Meteorologie coupled global climate model (MPI-ESM-LR, MPI hereafter; http://www.mpimet.mpg.de/en/science.htm), with the atmospheric component operating at T63 with a quadratic transform grid of ~1.9°, and 47 vertical levels. The second one is the Hadley Global Environmental 2—Earth System (HadGEM2-ES, HadGEM2-ES hereafter, https://verc.enes.org/models/earthsystem-models/hadgem2-es), with atmospheric resolution of N96 (approximately 1.875° × 1.25°), with 38 vertical levels and an ocean resolution of 1° (increasing to 1/3° at the equator) and 40 vertical levels. The first 5 years are discarded as model spin up allowing land-surface conditions to adjust while the period 1976–2005 is analyzed as reference period, i.e. present-days (RF) for models evaluation and on the other hand the period 2071–2100 is referred as the future period, i.e. late tewnty-first century. The difference between mean seasonal climatology of future and present days simulations is used to represent the model responses to GHGs forcing.

After a series of preliminary experiments, two different RegCM4 physics configurations were selected when nesting within the different AOGCMs in order to optimize the model performance (Mariotti et al. 2014). Their main

Table 1 RegCM4 configurations for the Africa-CORDEX simulations analysed in this paper

	HA_RegCM4	MPI_RegCM4
Number of levels	18	18
Horizontal resolution	50 km (0.44°)	50 km (0.44°)
Radiation scheme	NCAR CCM3 (Kiehl et al. 1996)	NCAR CCM3 (Kiehl et al. 1996)
Bondary layer scheme (PBL) scheme	Holstag PBL (Holstag et al. 1990)	Holstag PBL (Holstag et al. 1990)
Land surface scheme	CLM3.5 (Oleson et al. 2008)	BATS (Dickinson et al. 1993)
Large-Scale Precipitation scheme	SUBEX (Pal et al. 2000)	SUBEX (Pal et al. 2000)
Ocean scheme	Zeng (Zeng et al. 1998)	Zeng (Zeng et al. 1998)
Convection scheme	MIT-Emanuel (Emanuel 1991) over Ocean/ Grell (Grell et al. 1994) over Land.	Grell (Grell et al. 1994) for both Ocean and Land.
Initial and lateral boundary conditions	HadGEM2-ES	MPI-ESM-LR
Historical period (reference)	01st January 1970 till 31st December 2005	01st January 1970 till 31st December 2005
Future climate projection under RCP8.5 emission scenario	01st January 2006 till 31st December 2100	01st January 2006 till 31st December 2100

characteristics and physical parameterizations are presented in Table 1 and will be briefly described in the following.

For the HadGEM2-ES driven RegCM4 experiments (HA_RegCM4 hereafter), the land surface processes in RegCM4 are represented by the Community Land Model version 3.5 (CLM 3.5; Oleson et al. 2008) while convective precipitation is described by a mixed convection schemes employing the MIT convection parameterizations of Emanuel [Emanual (1991); Emanuel and Zivkovic-Rothman (1999)] over ocean and the scheme of Grell et al. (1994) over land areas.

For the MPI driven RegCM4 simulation (MPI_RegCM4 hereafter), RegCM4 was integrated over the same domain. In fact in MPI_RegCM4 simulation, the land surface processes are represented by the Biosphere–Atmosphere Transfer Scheme (BATS; Dickinson et al. 1993) whereas convective precipitation is represented via the scheme of Grell et al. (1994) over both land and ocean areas. Our present study focuses on the West African region (Fig. 1b) which has a complex topography, namely Cameroun Mountains (CM; Cameroun), Joss plateau (JP; Central Nigeria) and Guinea highlands (GH; Guinea) and is mainly characterized by the West African monsoon systems. In addition the regional analysis is performed over four selected sub-regions (Fig. 1b), which are here referred to as Western Sahel (WS), Sahel, Guinea and whole West Africa. Note however, that for the regional analysis such as the seasonal cycles and interannual variability as well as time series plots, both modeled and observed precipitation values were calculated taking into account land-only grid points.

2.2 Validation data

The reliability of climate experiments results is mainly based on the skill of climate models in reproducing the observed mean climate. Generally, Africa lacks high quality observation datasets at suitable temporal and spatial resolution necessary for rigorously assessing the skill of climate models simulations. For instance when comparing TRMM, GPCP and FEWS, Sylla et al. (2013b) pointed out significant discrepancies between these products whilst Nikulin et al. (2012) as well as Diallo et al. (2013a) found large differences between gauge-based observations and satellite products.

Based on this, the model mean climate is validated against observational datasets from different sources: (1) the monthly mean precipitation dataset at 0.5° × 0.5° resolution from the University of Delaware (UDEL, version 2.01; available from 1900 to 2010; Legates and Willmott 1990); (2) The 0.5° resolution monthly mean of precipitation from the latest version of the Climate Research Unit version 3.2 from the University of East Anglia (CRU TS3.2; http://badc.nerc.ac.uk/browse/badc/cru/data/cru_ts/cru_ts_3.20/data/; available from 1901 to 2011; Harris et al. 2013); (3) the monthly mean precipitation at the 2.5° × 2.5° horizontal resolution from the Global Precipitation Climatology Project version 2.2 (GPCP V2.2; Adler et al. 2003; available from 1979-to present) and iv) the monthly mean precipitation at 0.25° × 0.25° resolution from the Tropical Rainfall Measuring Mission (TRMM VB42V47, available from 1998 to present; Huffman et al. 2007). The large-scale atmospheric fields, which include the zonal and meridional wind as well as the mean sea level pressure (mslp) simulated by models, are compared with the pseudo-observed European Center for Medium-Range Weather Forecast (ECMWF; 1.5° × 1.5° resolution; Dee et al. 2011) reanalysis data ERA-Interim. In addition datasets from the National Centers for Environmental Prediction/National Center for Atmospheric Research (NCEP/NCAR) atmospheric reanalysis project 2 (R-2) with a

horizontal resolution of 2.5° × 2.5° (Kanamitsu et al. 2002) and available from 1948 to present are also used in this study.

We employ the satellite-based daily precipitation data at 0.25° × 0.25° horizontal resolution from the Tropical Rainfall Measuring Mission (TRMM VB42V47; Huffman et al. 2007; hereafter referred to as TRMM and available from January 1998-to December 2009) and the One-Degree Daily (1DD) data of GPCP V1.2 (Horizontal resolution is one degree in longitude and latitude; hereafter referred to as GPCP and available from October 1996 to December 2009) compiled by Huffman et al. (2009) to evaluate the model's performance to reproduce the present-day daily precipitation extreme indices. The reference period for the model evaluation is 1976–2005, while for the extreme indices assessment the reference period is compared, against the 1998–2009 period corresponding to the common period across the two satellite-estimate data. We recall that, for the interest of comparisons, we have interpolated both the validation datasets and model outputs onto the GPCP grid through a bilinear interpolation method.

2.3 Methodology

In this paper for the model's assessment, precipitation and large scale circulations parameters (wind and mean sea level pressure) climatology, as well as rainfall interannual variability and daily precipitation extreme indices, are only analyzed for the main peak of the WAM season, i.e. June–July–August–September (JJAS). However, the seasonal cycle considers the monthly climatology averaged over the Sahel, West Sahel, Guinea and entire West Africa as shown in Fig. 1. The precipitation interannual variability over different sub-regions are assessed using the coefficient of variation, i.e. the standard deviation divided by the mean precipitation, in order to remove the dependence of the precipitation standard deviation from the mean (Giorgi 2002). In addition, we should keep in mind that, the regional average values are obtained after first calculating the coefficient of variation at the individual grid point and then averaging over the region's area. Note, however that the assessment of mean seasonal biases of surface variables obtained from these simulations are presented in Coppola et al. (2014).

2.3.1 Precipitation indices

Four mains indicators of climate extremes based on daily precipitation are evaluated for their direct impacts on water resources and agricultural productivity. Their definitions as detailed below follow that of Tebaldi et al. (2006), Diallo et al. (2015) and Sillmann et al. (2013a, b) and are calculated on JJAS seasonal basis.

- Frequency (Freq): defined as the number of days with rainfall amount >1.
- Heavy precipitation day's event (R10mm): defined as number of days with daily precipitation greater than or equal 10 mm ($R_{day} \geq 10$ mm).
- Maximum 5 day precipitation (RX5day): defined as the maximum of 5 day precipitation accumulations.
- Consecutive dry days (CDD): defined as the maximum number of consecutive dry days with daily rainfall below 1 mm, i.e. days with rainfall amount <1 mm ($R_{day} < 1$ mm). The CDD is the length of the dry spell.

The SDII (Simple daily intensity index: mean daily precipitation intensity during wet days), RX5day and R10mm express the intensity and the precipitation frequency.

2.3.2 Water budget analysis

To understand the change in the hydrological cycle we employed the atmospheric water budget equation suggested by Peixoto and Oort (1992) and expressed as:

$$\left\langle \frac{\partial W}{\partial t} \right\rangle + \langle D \rangle = \langle E - P \rangle \tag{1}$$

where E is evaporation, P is the precipitation, W is the atmospheric water vapor storage, D is the divergence of the vertically integrated moisture flux and angled brackets denotes the area average. The terms W and D are defined by:

$$W = \frac{1}{g} \int_{Pt}^{Ps} q dp$$

$$D = \nabla.Q \quad \text{where} \quad Q = \frac{1}{g} \int_{Pt}^{Ps} qv dp$$

q is the specific humidity (g/kg), V is the horizontal wind vector (m/s), P_s is the pressure (hPa) at surface level, P_t is the pressure at the top of the atmospheric layer considered and g (N/kg) is the gravitational acceleration. In JJAS, over WA, the monsoon flow occurs primarily below 700 hPa and the African Easterly Jet (AEJ) is centered at 600 hPa. This motivates a decomposition of the atmospheric column moisture transport into an integral from the surface pressure level to 850 hPa, i.e. 1000–850 hPa (bottom level hereafter) and from 850 to 300 hPa (upper levels hereafter).

On longer time interval like monthly or seasonal in near equilibrium conditions, the change in storage of water vapor term i.e. $\frac{\partial W}{\partial t}$ is usually small compared to the magnitude of large-scale convergence and evaporation (Oki et al. 1995; Trenberth 1999; Senevirante et al. 2004). Thus Eq. (1) describing the atmospheric water budget can be approximately written as,

$$\langle E - P \rangle = \langle \nabla.Q \rangle \tag{2}$$

Equation (2) is therefore an indicator of water vapor sources (evaporation exceeds precipitation) and sinks (precipitation exceeds evaporation) (Chen et al. 1988). We obtain E, P as well as low and upper level Q from our simulations and calculate their difference over different JJAS seasons. Moreover we also used the meridional wind (v-wind) and the vertical wind (omega) profile as well as the AEJ, i.e. the zonal wind at 600 hPa to seek the associated change in atmospheric dynamic to the late twenty-first century change in hydrological cycle. It is noteworthy that the assessments of certain hydrological cycle components are presented in Diallo (2015). Thus to avoid repetition and for brevity, in this paper after the model evaluation, we then focused on the projected change in rainfall extreme events and the hydrological cycle components as well as possible mechanisms underlying changes over the WA region.

3 Result and discussion

3.1 Model evaluation

In this section, we present a brief assessment of the two RegCM4 (MPI_RegCM4 and HA_RegCM4) reference simulations and the two driving Earth System Models (ESMs; HadGEM2-ES and MPI-ESM) historical simulations in reproducing the main features of the WAM mean precipitation, atmospheric circulation, rainfall interannual variability and different hydroclimatic indices (defined in Sect. 2.3.1).

3.1.1 Mean rainfall and low-level circulation patterns

Figure 2a–h shows the mean JJAS seasonal precipitation climatology from CRU, UDEL, GPCP, TRMM, HadGEM2-ES, MPI, HA_RegCM4 and MPI_RegCM4. Data from CRU, UDEL and all models are averaged for the period 1976–2005 whilst the GPCP average corresponds to the period 1979–2005 the TRMM data over 1998–2009. Note that, the periods for the different datasets are slightly different, however, recently Giorgi and coauthors (2014) argued that this is not likely to affect the first order comparison presented here, which is based on statistics over the entire periods. Table 2 summarizes the JJAS quantitative metrics of differences across models and observation estimates calculated for the whole West Africa, Guinea, Sahel as well as West Sahel sub-regions. The spatial distribution of precipitation from observations (CRU, UDEL, GPCP and TRMM; Fig. 2a–d) locate the Intertropical Convergence Zone (ITCZ, i.e. band of high rainfall intensity) in a wide zonal band between 6° and 14°N with rainfall intensities decreasing either going northward or southward of this band. Observations show three peaks of rainfall maximum

around the Guinea highlands, Jos plateau in central Nigeria and Cameroon Mountains. Close examination of observations shows some spatial pattern differences between them. For instance GPCP has a narrower area of maximum along the coastlines of Cameroun/Nigeria highlands whereas CRU and UDEL show a discontinuity in the band of high rainfall intensity.

Both ESMs (Fig. 2e, f) reproduce the general geographical patterns of the observed rainfall distribution (PCC greater than 0.70, see Table 2), though MPI shows a slight overestimation of the intensities over the ITCZ (Fig. 2f) whereas HadGEM2-ES fails to move the precipitation far enough northward over the Sahel (Fig. 2e), in accordance with the underestimation of the temperature gradient between the Sahara and the Gulf of Guinea (not shown, see Coppola et al. 2014 and Diallo 2015). A common feature among the ESMs is the bias maxima off the coast in the eastern Atlantic and the Gulf of Guinea, probably resulting from their failure to fully transport the moisture from the ocean inland. In fact, a similar bias was reported by Laprise et al. (2013). In their study, they associated the wet bias in ESMs over the Gulf of Guinea to the simulated SST biases in this region leading to a rainfall reduction over Sahel as illustrated in Fig. 2e. HA_RegCM4 and MPI_RegCM4 (Fig. 2g, h) reasonably reproduce the main band of high rainfall and replicate better the orographic rainfall in complex terrain compared to the driving ESMs, especially over the Guinean highlands and Jos plateau, resulting in a better PCC over Guinea and MAB not exceeding 11 % over Sahel (Table 2). The RegCM4 simulations exhibit therefore important improvements compared to the driving ESMs, highlighting thus substantial added value in the use of RegCM4 (e.g. Coppola et al. 2014; Diallo et al. 2015).

This indicates that although the large-scale environment plays an important role in regional climate model (RCM) simulations, the RCM internal dynamics is a keys element for rainfall simulation due to a better representation of smaller scale topographic forcing and local land surface processes. In addition, HA_RegCM4 is found to perform better compared to MPI_RegCM4 and has a spatial pattern which is largely more consistent to that of different observations. Thus, the differences between the two RegCM4 simulations may likely arise either from the driving boundary conditions or/and to the difference in land surface scheme which is an important element in simulating the West African monsoon (e.g. Steiner et al. 2009; Ruti et al. 2011). Furthermore, the tendency of models to simulate higher/lower precipitation may probably arise from a poor simulation of the large scale circulation patterns.

Figure 3a–f displays the mean climatological pattern of JJAS mean sea level pressure (mslp) superimposed to the low-level 925 hPa winds obtained from ERA-Interim, NCEP reanalysis, HadGEM2-ES, MPI, HA_RegCM4 and

Fig. 2 Mean JJAS rainfall (in mm/day) from: **a** CRU, **b** UDEL, **c** GPCP, **d** TRMM, **e** HadGEM2-ES, **f** MPI, **g** HA_RegCM4, and **h** MPI_RegCM4. The means is calculated using the 1976–2005 period except for GPCP and TRMM, for which the 1979–2005 and 1998–2009 periods are used respectively
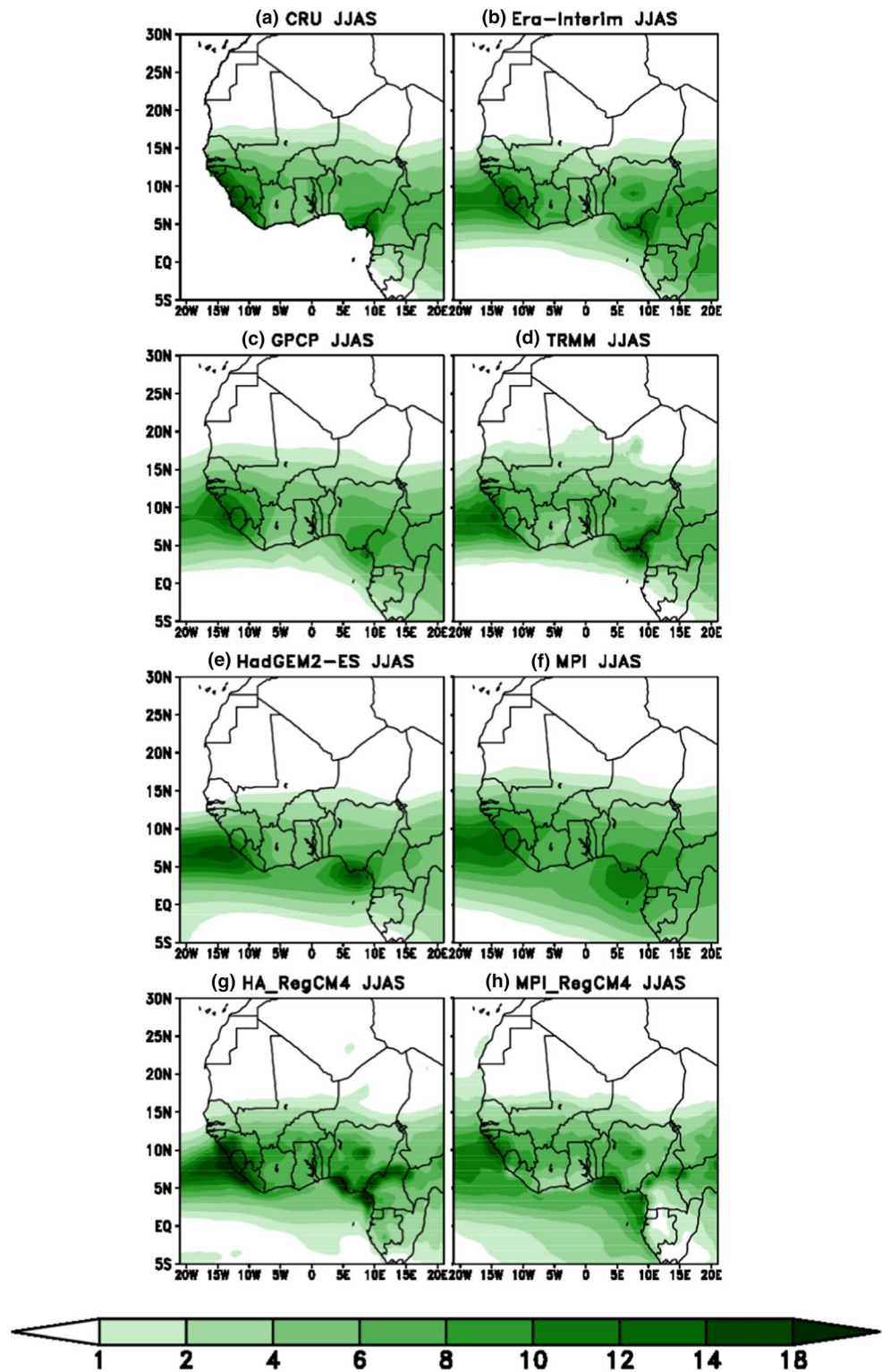
MPI_RegCM4. The data for the NCEP reanalysis and the models are averaged for the period 1976–2005 whereas in ERA-Interim the average covers the period 1979–2005. Both the NCEP and ERA-Interim reanalysis have areas of low mean sea level pressure over the Sahara desert between 17° and 27°N coinciding with the area of maximum 2 m temperature in observations (not shown) and corresponding to the Saharan heat low (SHL). The southwesterly winds driven by the surface pressure gradient between the Gulf of Guinea and Sahara reach north of 20°N in the reanalysis.

Table 2 Mean Absolute Bias (MAB) and the Pattern Correlation Coefficient (PCC) between simulated precipitation and the CRU observation

	Sahel		West Sahel		Guinea		West Africa	
	Mean Bias (%)	PCC	Mean Bias (%)	PCC	Mean Bias (%)	PCC	Mean Bias (%)	PCC
GPCP	2.18	0.98	2.62	0.99	9.76	0.92	5.64	0.97
TRMM	6.11	0.94	1.02	0.97	5.81	0.95	4.74	0.96
HadGEM2-ES	19.27	0.74	16.36	0.86	10.32	0.76	14.75	0.73
HA_RegCM4	9.04	0.95	4.19	0.90	8.55	0.80	8.38	0.81
MPI	13.32	0.88	12.68	0.81	13.85	0.72	−10.35	0.79
MPI_RegCM4	10.18	0.97	10.22	0.84	9.48	0.78	−10.35	0.93

The key monsoon features present in the reanalysis are reasonably reproduced in all models, though some deficiencies are still evident in both ESMs and RCMs. HA_RegCM4 and MPI_RegCM4 underestimate the mean sea level pressure over the Sahara, inducing a stronger pressure gradient between the Sahara and Gulf of Guinea which results in strong inland moisture penetration and a better representation plus some overestimation of ITCZ rainfall compared to the driving ESMs (Fig. 2g–h). Both ESMs show some slight displacements in the location of the low surface pressure area, which covers a wider and tilted region encompassing the whole Sahara and eastern Sahel. Diallo (2015) and Coppola et al. (2014) found that in HadGEM2-ES the maximum 2 m-temperature over the Sahara is underestimated and extended southward of the observed location. Thus, the southward extension of the SHL in HadGEM2-ES (Fig. 3c) results from the southward position of the low pressure center which inhibits moisture advection by preventing the monsoon flow to extend far enough to the north (see Fig. 2e).

These shortcomings in the large scale circulation over the region are considerably improved when RegCM4 is driven either by HadGEM2-ES or MPI, resulting to the better representation of precipitation in both HA_RegCM4 and MPI_RegCM4 as discussed earlier. It should be noted that RegCM4 improves the simulation of the African Easterly Waves (AEWs) activity, compared to both driving AOGCMs (e.g. Mariotti et al. 2014), as well as the location and intensity of the African Easterly Jet (AEJ) and Tropical Easterly Jet (TEJ) (Diallo 2015).

3.1.2 Mean annual cycle and interannual variability

Figure 4 presents the area-averaged (land-only grid point) of observation-based and simulated rainfall seasonal cycle for the selected sub-domains highlighted in Fig. 1. While acknowledging the observational uncertainty over different sub-regions, both the global and regional models reproduce fairly well the annual cycle over the main Sahel and West Sahel regions (Fig. 4a, b), with RegCM4 outperforming the

corresponding driving ESMs. The dry season from November to March is well simulated by the models as is the timing of the peak in August, and the subsequent rapid decline. HadGEM2-ES generates too little rainfall in the main rainy season (June to September) over both sub-regions. This bias can be attributed to the southward position of the ITCZ rain-band discussed earlier (see Fig. 2e). The RegCM4 simulations generate more rainfall than corresponding driving ESMs, specifically around the season peak (August) in West Sahel, and compare better with GPCP, CRU and TRMM.

Over the Guinea region (Fig. 4c), UDEL, GPCP and TRMM show a bimodal distribution of rainfall associated with the meridional progression and retreat of the tropical rain-belt (so called ITCZ) over land. The first rain maximum occurs in June and the second one in September with a minimum around July–August corresponding to the rainy season over the Sahel. Relative to CRU, GPCP and UDEL, TRMM underestimates rainfall amounts throughout the year, but captures fairly well the timing of rainfall maxima. The Rainfall amounts from HA_RegCM4 and MPI_RegCM4 are similar to each other in most of the seasons despite the different lateral boundary information, suggesting a dominant role for model physics over the lateral boundary forcing. RegCM4 overestimates the rainfall amounts compared to the ESMs and observations (i.e. CRU, UDEL, GPCP and TRMM), and the timing of the second rainfall peak (September) agrees with observations. HadGEM2-ES does not capture the bimodal distribution of the Guinean seasonal cycle and underestimates rainfall over the West Africa sub-region (Fig. 4d).

The precipitation coefficient of variation (CV) obtained from observations (CRU, TRMM and GPCP) and both ESMs and corresponding RegCM4 experiments averaged over the four sub-regions are presented in Fig. 5. In all sub-regions, TRMM (GPCP) provides the largest (lowest) values of the interannual variability, likely as a result of its higher resolution (Giorgi 2002), and RegCM4 values are closer to TRMM. In fact, both the global and regional models tend to simulate variability within the range of the

Fig. 3 Mean JJAS seasonal distribution of mean sea level pressure (mslp; expressed in hPa) superimposed to the low level (925 hPa) wind vector (expressed in m/s) from: **a** NCEP, **b** ERA-Interim, **c** HadGEM2-ES, **d** MPI, **e** HA_RegCM4, **f** MPI_RegCM4. The mean is calculated using the 1976–2005 period except for ERA-Interim, for which the period 1979–2005 is used
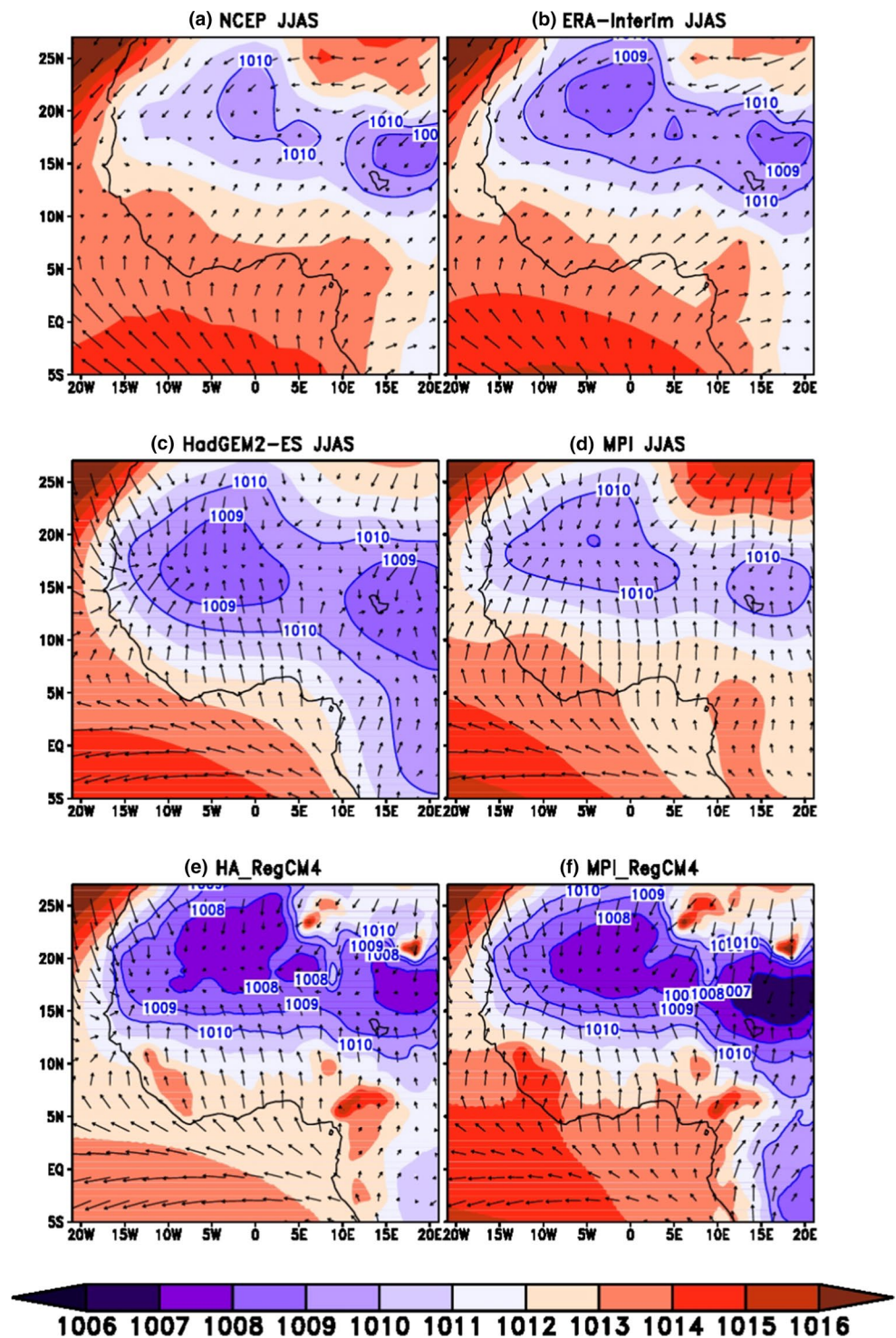
observations, with larger values of CV in the RegCM4 experiments compared to the ESMs, likely due to the higher resolution (Giorgi 2002). We also note that over both the Sahel and West Sahel, the RegCM4 interannual variability values tend to be closer to the driving ESMs than over the Guinea region, suggesting a more important role of the forcing ESMs.

3.1.3 Extreme indices

Figure 6 shows the precipitation frequency (i.e. the number of days with precipitation higher than 1 mm; Fig. 6a–f) and the R10mm (number of days with precipitation greater than or equal 10 mm day^{-1}; Fig. 6g–l) obtained from GPCP, TRMM, ESMs and RegCM4 experiments. GPCP
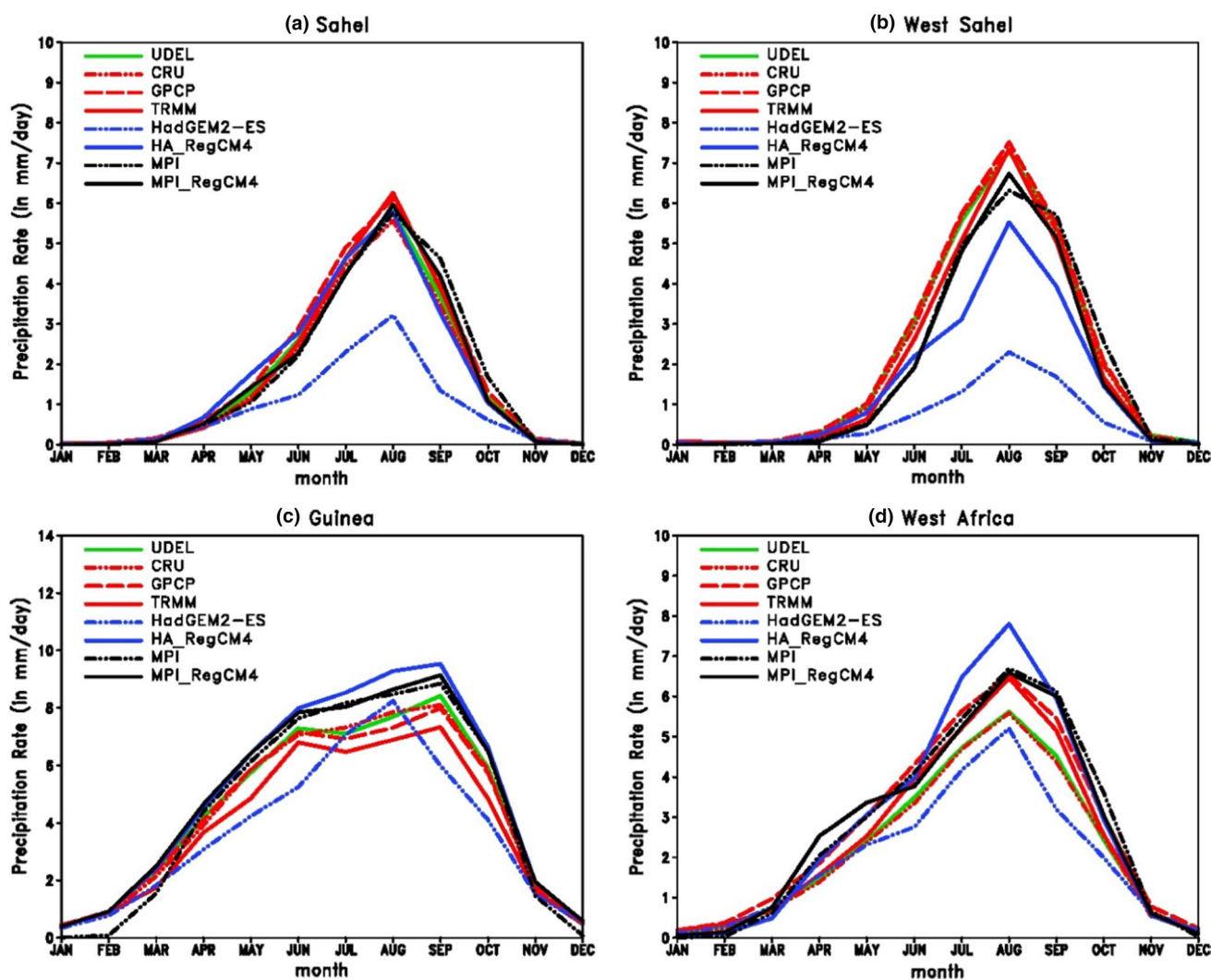
Fig. 4 Mean annual cycle of monthly precipitation (in mm/day) over: **a** the Sahel, **b** the West Sahel, **c** the Guinea region and **d** the West Africa region for CRU, UDEL, GPCP, TRMM, HadGEM2-ES, MPI, HA_RegCM4, and MPI_RegCM4. The means is calculated using the 1976–2005 period except for GPCP and TRMM, for which the 1979–2005 and 1998–2009 periods are respectively used

and TRMM show large number of events along the ITCZ and over orographic regions, with decreasing gradients north and south of the band of maximum events. However, GPCP shows greater frequency, specifically over the Guinean highlands and the border Nigeria/Cameroon, due to its coarser resolution. The spatial patterns of R10mm are consistent across the two observation products, with largest values coinciding with areas of highest frequency. There is a disagreement between observation-products, especially along the ITCZ rain-band, where GPCP exhibits larger numbers of R10mm events, most likely due to the higher precipitation frequency in this areas (see Fig. 6a). Both global and regional models reproduce the overall pattern of mean frequency and R10mm events, although the global models overestimate the frequency along the ITCZ rain-band, especially HadGEM2-ES, which can likely

be a result of too many drizzle events. Conversely, both RegCM4 experiments show a good agreement with the TRMM observations. For instance, HadGEM2-ES (MPI) underestimates (overestimates) the mean R10mm (frequency) events along the ITCZ rain-band, where RegCM4 experiments show values more in line with TRMM, emphasizing the added value of the downscaling exercise.

Other important aspects of daily precipitation characteristics for evaluating climate variability and impacts are the maximum amount of rainfall during 5 day periods (RX5day) and dry spells length (CDD) within the monsoon season. Figure 7 shows the patterns of RX5day (Fig. 7a–f) and CDD (Fig. 7g–l) for observations, global models and RegCM4 experiments. First, we find a disagreement in terms of RX5day between the observation products, with GPCP missing in particular the maxima over topographic areas. Both

Fig. 5 Coefficient of variation (CV, in %) for precipitation in the 4 sub-regions: **a** Sahel and West Sahel, **b** Guinea and West Africa for CRU, GPCP, TRMM, HadGEM2-ES, MPI, HA_RegCM4 and MPI_RegCM4. The means is calculated using the 1976–2005 period except for GPCP and TRMM, for which the 1979–2005 and 1998–2009 periods are respectively used
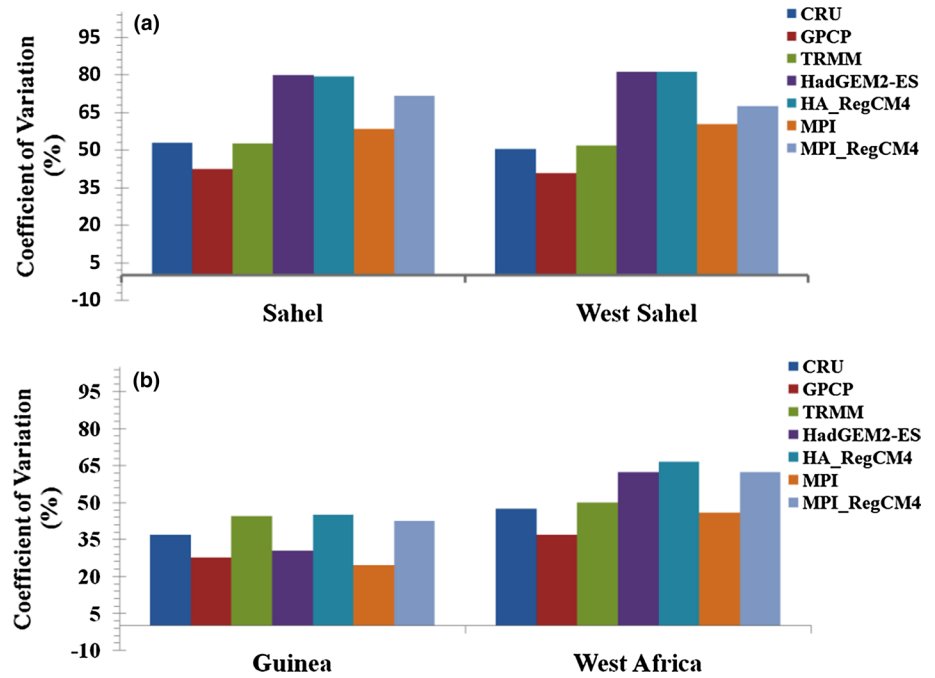
global and regional models reproduce reasonably well the overall patterns, with the ESMs being closer to GPCP and the RegCM4 experiments to TRMM. In fact, common deficiencies in HA_RegCM4 and MPI_RegCM4 are an overestimation of the RX5day along the Soudano-Sahelian region and an underestimation over the Cameroon Mountains.

The spatial patterns of the average dry spell length (Fig. 7g–l) show a good general agreement across the different RegCM4 experiments, ESMs, and observations. As expected, the shortest dry spell length is found along the ITCZ band and regions of complex topography and the longest spells south and north of it. Both global and regional models realistically reproduce the patterns of the CDD, though few shortcomings are still evident. For instance, HadGEM2-ES and MPI overestimate the spells over the Sahel and flatter terrains of Guinea region, while the RegCM4 experiments overestimate the shortest dry spells further east over Niger/Nigeria because of more frequent rainfall events and maximum RX5day in these areas.

In summary global and regional models reproduce reasonably the different precipitation extreme indices though some shortcomings are still evident, with AOGCMs showing better agreement with GPCP and RegCM4 comparing better to TRMM.

3.2 Climate change projections

3.2.1 Mean precipitation

The projected mean precipitation change from HadGEM2-ES, MPI, HA_RegCM4 and MPI_RegCM4 are presented

in Fig. 8. A consistent pattern of change signal off the western African coasts, in the western Sahel (westward 5°W) over Senegal, Mauritania and more largely over regions south of 5°N emerges, consisting of a pronounced decrease of more than 40 % in precipitation for HA_RegCM4 as well as in MPI_RegCM4. These drier conditions are mostly associated to the large warming (up to 4°–6°, not shown) found there, probably a result of lower evaporative cooling and cloudiness. The decrease may likely be also induced in part by a weakening in moisture from local sources, thereby slowing down the hydrological cycle (Seth et al. 2013; Saeed et al. 2013; Li et al. 2015). The corresponding driving ESMs agree in showing this significant drying, along with a precipitation increase in eastern and/or central Sahel, and western Guinean coast. MPI_RegCM4 closely replicates this spatial distribution with more details whereas HA_RegCM4 shows drying conditions more extended over the Gulf of Guinea. Overall, the similarities found between the driving ESMs and nested RegCM4 suggest that over the western Sahel the negative changes are primarily driven by the large-scale environment described by the lateral boundary forcing. Conversely, the marked differences between the ESMs and RegCM4's projections over other areas highlight the role of local conditions in modulating the response of the regional climate to the increasing GHGs forcing. These changes in mean precipitation likely have substantial impacts on the changes in extreme precipitation.

The JJAS projected change in frequency of daily events and in R10mm obtained from HadGEM2-ES, MPI, HA_RegCM4 and MPI_RegCM4 are presented in Fig. 9a–h; whilst Fig. 10a–h show the projected changes for the
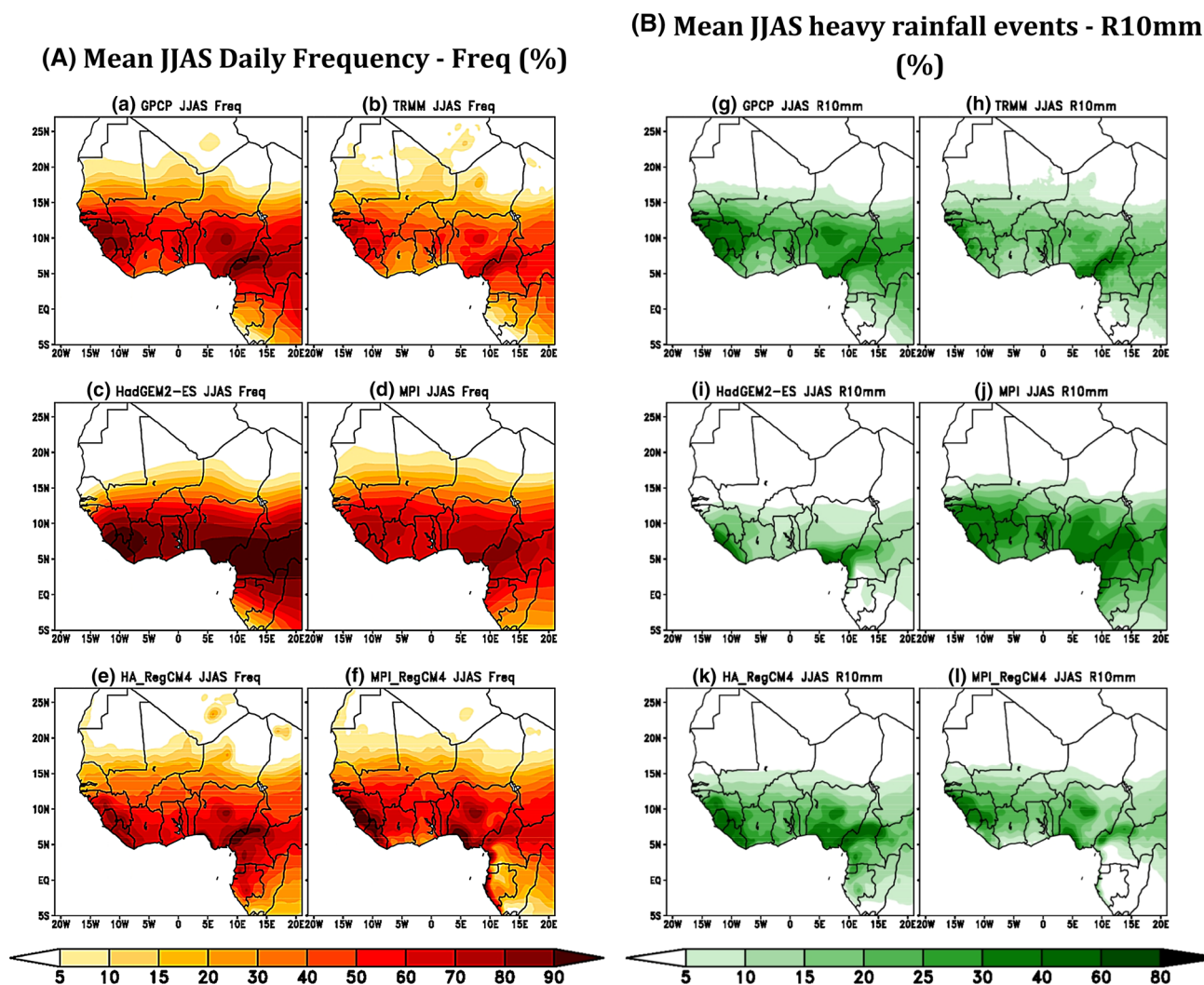
(A) Mean JJAS Daily Frequency - Freq (%)

(B) Mean JJAS heavy rainfall events - R10mm (%)

Fig. 6 Average JJAS mean daily frequency—Freq [**A**], in %] and mean heavy rainfall events—R10mm [**B**], %] from: GPCP (**a**, **g**), TRMM (**b**, **h**), HadGEM2-ES (**c**, **i**), MPI (**d**, **j**), HA_RegCM4 (**e**, **k**), MPI_RegCM4 (**f**, **l**). Models are averaged for the 1976–2005 period while TRMM and GPCP averages cover the 1998–2009 periods

RX5day and dry spell length (CDD). Generally, the pattern of change in frequency, R10mm and RX5day follows the change in mean precipitation, indicating that changes in extreme and mean precipitation share common features. We also note, however that the area of increased (decreased) RX5day are more (less) extended than those of increased mean precipitation, and conversely the area of increased (decreased) frequency and R10mm events are less (more) extended than those of mean precipitation. This implies that the models show a trend towards a regime of more intense and less frequent extreme rainfall events under global warming conditions which is in agreement with previous findings (e.g. Trenberth 2011; Giorgi et al. 2011, 2014). Thus the precipitation increases in eastern and/or central Sahel is not only in the seasonal mean but also in the RX5day. On the other hand, the areas where CDD

(Fig. 10e–h) increase coincide generally with the regions affected by a decrease in mean precipitation. In particular, significant increases of CDD occur in western Sahel, towards the Guinean regions as well as over high topography such as Guinean highlands, Cameroon Mountains and Jos plateau. It is worth pointing out that all models are in agreement in capturing the simultaneous decreases in the rainfall frequency and R10mm events projected over the Western Sahel, indicating that an increase in maximum dry spell length along with a decrease of high intensity precipitation events during the monsoon season are likely responsible for the projected dry conditions. Overall, changes in precipitation frequency and intensity distribution over West Africa will have a direct effect on dry spells sequences and therefore will affect various climate sensitive sectors such as rain-fed agriculture.
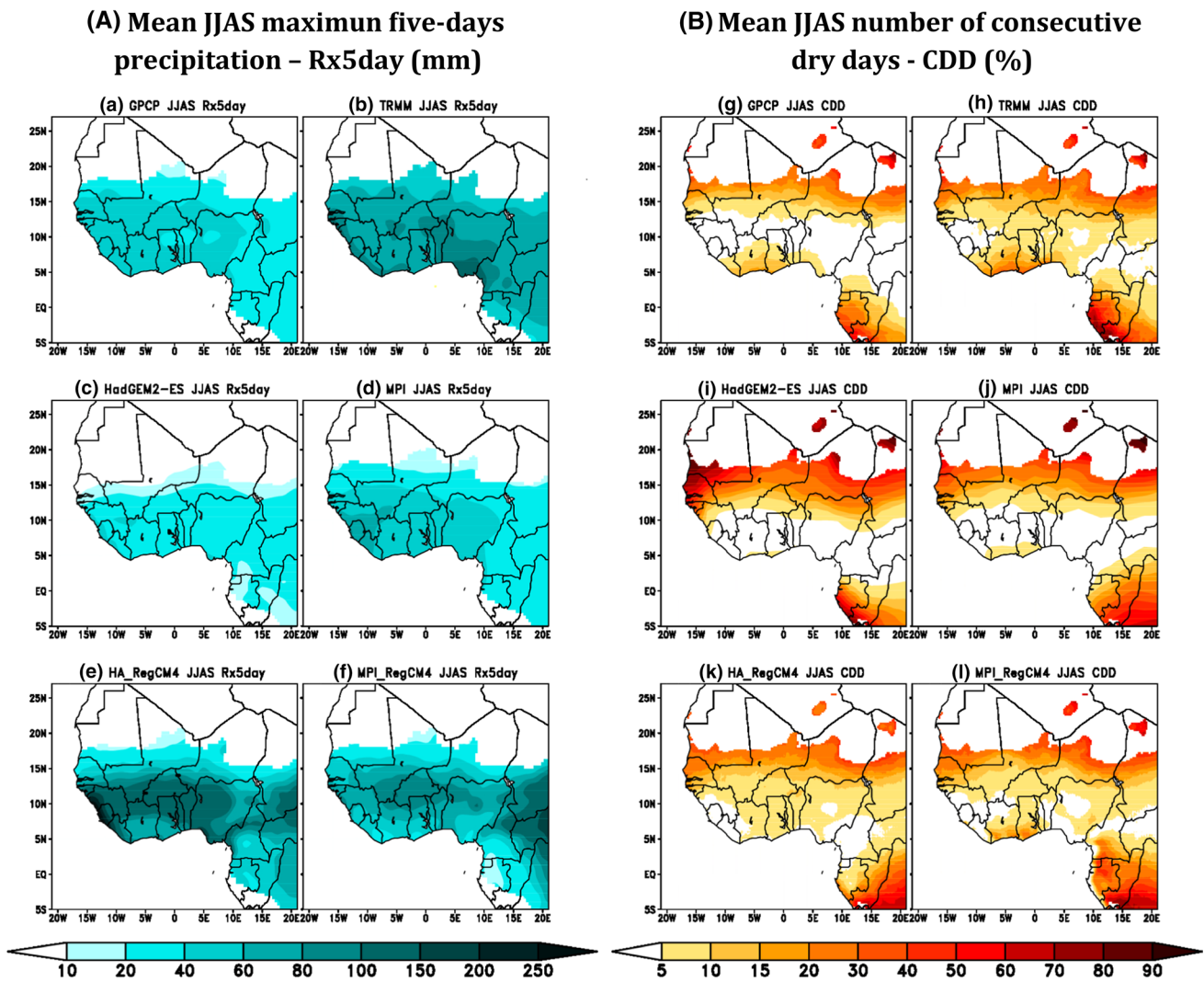
(A) Mean JJAS maximun five-days precipitation – Rx5day (mm)

(B) Mean JJAS number of consecutive dry days - CDD (%)

**Fig. 7** Average mean JJAS maximum-5 days precipitation—RX5day [**A**], mm] and maximum number of consecutive dry days (i.e. dry spells length)—CDD [**B**], in %] from: GPCP (**a**, **g**), TRMM (**b**, **h**), HadGEM2-ES (**c**, **i**), MPI (**d**, **j**), HA_RegCM4 (**e**, **k**), MPI_RegCM4 (**f**, **l**). Models are averaged for the 1976–2005 period while TRMM and GPCP averages cover the 1998–2009 periods

To further investigate the link between the mean precipitation change and the monsoon season over the Western Sahel region highlighted in Fig. 1b, we performed an area average (land point only) of precipitation, frequency, CDD and RX5day over the region. Figure 11a shows the seasonal cycle of precipitation over the western Sahel averaged for the reference (1976–2005) and the late future (2071–2100) periods. We first note that, in general, models project precipitation to decrease throughout the year, with the largest decrease during the JJAS monsoon season. Moreover, all models predict a monsoon onset delay which is followed by an early withdrawal of the ITCZ rain-band in the late twenty-first century, resulting then in a shortening of the monsoon season. In agreement with previous studies, these results indicate both a delay and a shortening in the monsoon rainy season in response to increasing GHG

concentrations (Diallo et al. 2012; Mariotti et al. 2014; Seth et al. 2013).

To gain an insight on whether the weakening of the monsoon season over the west Sahel is tied to possible changes in extreme events, we show in Fig. 11b–e the JJAS time series change relative to the 1976–2005 reference period of mean precipitation, frequency, CDD and RX5day averaged over the region from early through the end of the twenty-first century, (2006–2100). The models show a marked decrease in mean monsoon precipitation, frequency and RX5day, particularly after 2070 (Fig. 11b, c, e). Furthermore, a decrease in both mean precipitation and frequency results into a significant increase in dry spells length (CDD), which again emphases the vulnerability of the region to drought conditions.

Fig. 8 Mean JJAS projected rainfall change [(2071–2100) minus (1976–2005)] from: **a** HadGEM2-ES, **b** MPI, **c** HA_RegCM4 and **d** MPI_RegCM4. The change is expressed in percent (%) with respect to the 1976–2005 reference periods
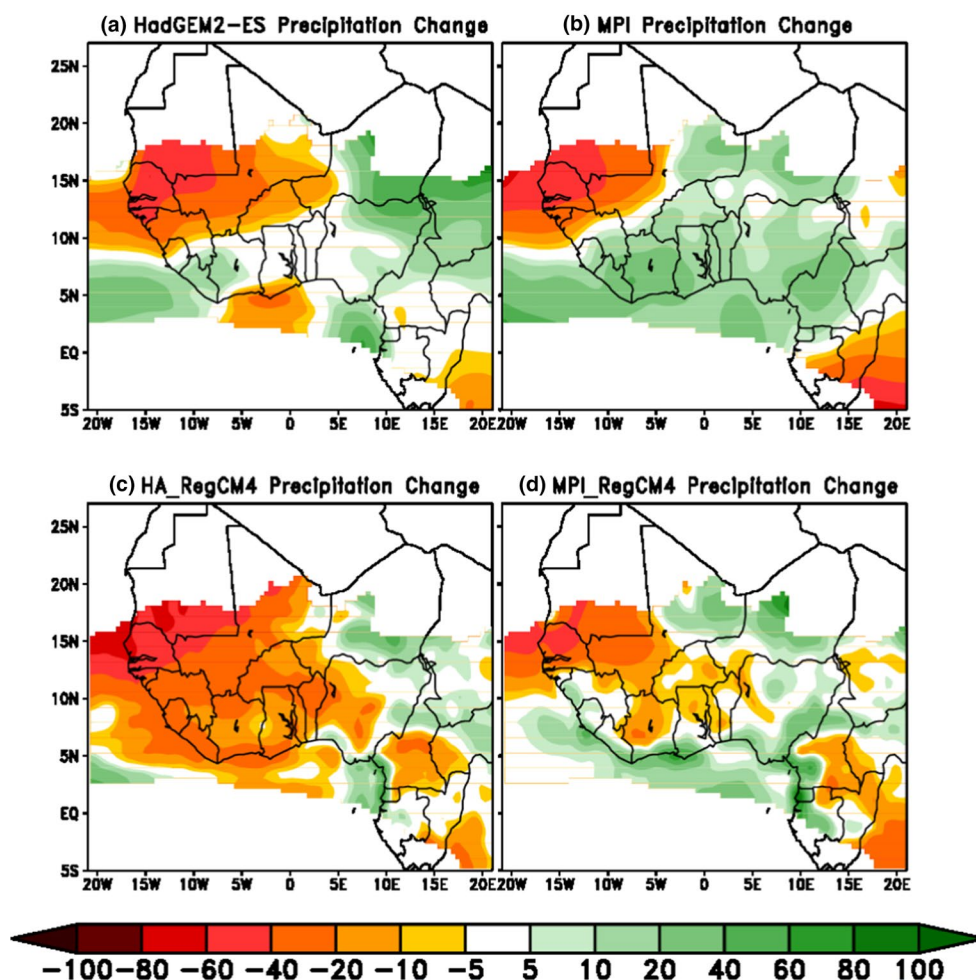
The West African climate is mainly driven by the WAM system. Thus it is useful to investigate the change in atmospheric circulation. The JJAS change in mslp and low level wind at 925 hPa in HA_RegCM4, MPI_RegCM4 (Fig. 12c, d) and also the driving ESMs (Fig. 12a, b) are displayed in Fig. 12. The models show that the SHL deepens by 1 hPa in the late twenty-first century, though mslp changes in the ESMs over the Sahel and Sahara are weaker. The high mslp over the Gulf of Guinea increases slightly. As a result of these mslp anomalies, the change in low level westerly flow do not penetrate deep into the western Sahel, but is diverted northward to the central and/ or eastern Sahara. Similar dynamical circulations in observations are associated with precipitation increases over central/eastern Sahel (e.g. Vellinga et al. 2013;Vizy et al. 2013; Diallo et al. 2014). Therefore, such changes are consistent with the wet conditions projected over the eastern Sahel. Furthermore, the main core of ascending air linked to the moist convective processes within the ITCZ and located around 9°N (e.g. Nicholson 2009, 2013; Diallo et al. 2014) weakens in the future in both HA_RegCM4 and MPI_RegCM4 (Fig. 13c, d) and is even replaced by

a deep core of subsidence extending between 3 and 13°N and maintained between the core of the AEJ and TEJ, consistent with the rainfall decrease over the western Sahel. In addition, the meridional wind in both RegCM4 simulations (Fig. 13a, b) is projected to increase in the high troposphere above 400 hPa around 10°N, indicating an enhancement of the northward Hadley cell branch. Thus, from this large scale dynamics change, the projected dryness in the western Sahel would be likely originated from a weakening of both atmospheric water vapor and low level westerly flux. As a result, these changes favor a weakening of the deep moist convection processes (Fig. 13c, d) which induce a rainfall inhibition. Therefore, the rainfall enhancement is probably tied to the increased moist flow penetrating into West Africa with an intensification of moisture convergence over the eastern and/or central Sahel and an enhancement of the northern Hadley cell.

In summary the western/eastern precipitation dipole pattern change in the Sahel is in agreement with recent studies using either CORDEX simulations (e.g. Mariotti et al. 2014; Laprise et al. 2013) or CMIP5 simulations (e.g. Monerie et al. 2012). Monerie et al. (2012) associated the
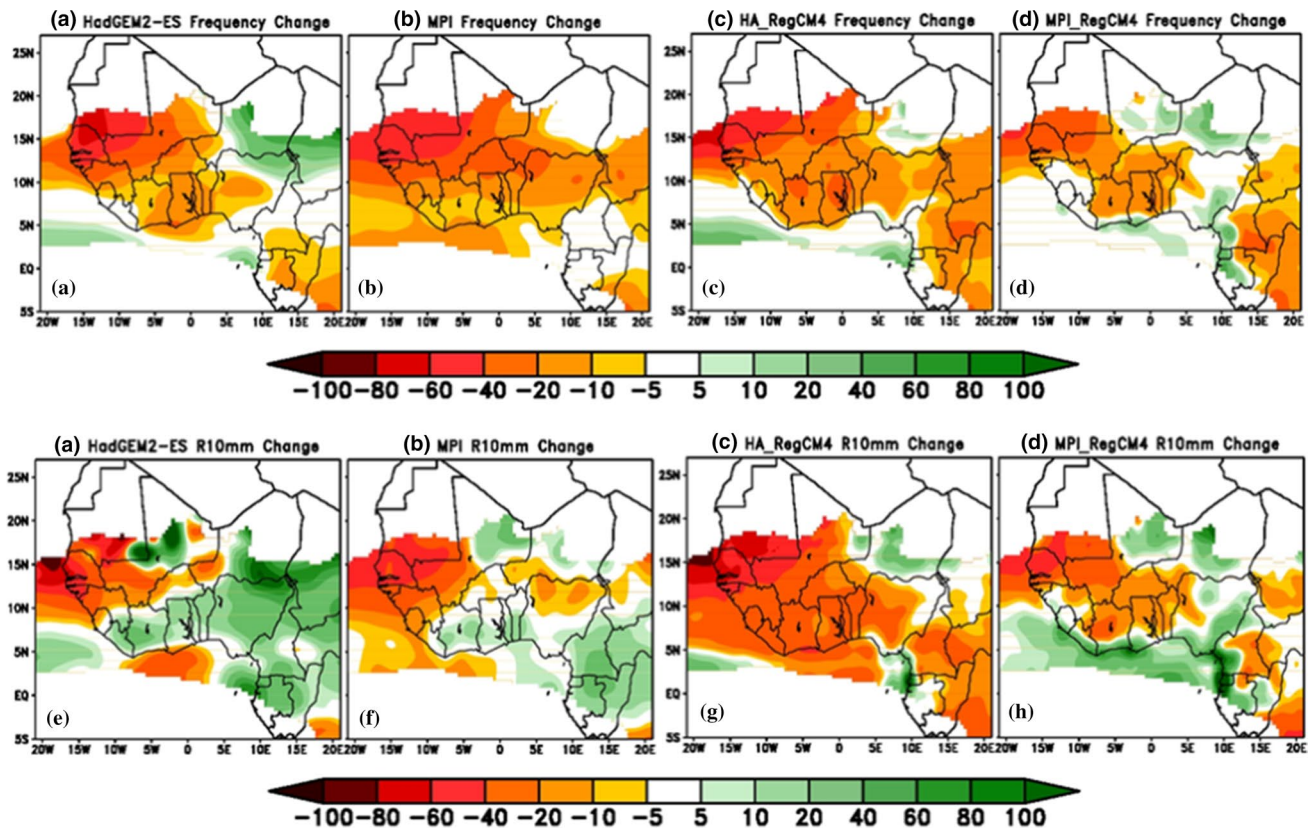
Fig. 9 Mean JJAS projected change [(2071–2100) minus (1976–2005)] in mean daily Frequency—Freq (*top panels*; **a–d**) and heavy rainfall events—R10mm (*bottom panels*; **e–h**) from: HadGEM2-ES (**a**, **e**), MPI (**b**, **f**), HA_RegCM4 (**c**, **g**) and MPI_RegCM4 (**d**, **h**). The change is expressed in percent with respect to the 1976–2005 reference periods

rainfall decrease to increased air subsidence, whereas on the other hand Mariotti et al. (2014) associated the precipitation decrease with a weakening of the 6–9 day regime of the AEWs activity.

In order to identify the source of projected precipitation differences among the models we analyzed the hydrological cycle over the region, focusing specifically on evaporation which should contribute to local precipitation changes.

3.2.2 Atmospheric water budget and moisture transport

Figure 14a–d shows the evaporation change obtained from HadGEM2-ES, MPI, HA_RegCM4 and MPI_RegCM4, while Fig. 14e–h displays the corresponding change in evaporation minus precipitation (E–P) obtained from the ESMs and RegCM4. In general, the pattern of mean evaporation change follows that of precipitation change, though some differences are evident among the models. HadGEM2-ES as well as HA_RegCM4 and MPI_RegCM4 predict an increase (decrease) in evaporation over eastern (western) Sahel, inducing enhanced (weakened) local recycling of moisture. Conversely, evaporation in MPI is projected to decrease by up to 40 % through the whole

Sahelian band, while it increases around the Cameroun Mountains. The reduced evaporation over the western Sahel enhances the sensible heat fluxes over the region and north Sahel, thereby raising the surface air temperature. It is worth pointing out that, as shown in Fig. 8, in some areas the precipitation decrease contributes to the evaporation weakening by reducing water availability, thus emphasizing that precipitation is important factor in determining the evaporation response. Furthermore, as expected all the water bodies, i.e. the Atlantic Ocean, show evaporation increases consistent with the surface temperature increases due to GHGs forcing. The above analyses suggest that under the RCP 8.5 scenario atmospheric water vapor and moisture transport can be major factors in determining precipitation changes over West Africa.

In general the precipitation pattern change depends on the balance between evaporation and precipitation which are the key water budget components. The balance between evaporation and precipitation from HA_RegCM4 as well as MPI_RegCM4, mostly shows a projected surplus (E > P) of moisture indicating that the atmosphere is gaining moisture from the underlying land. On the other hand, MPI mostly projects a moisture deficit (E < P),
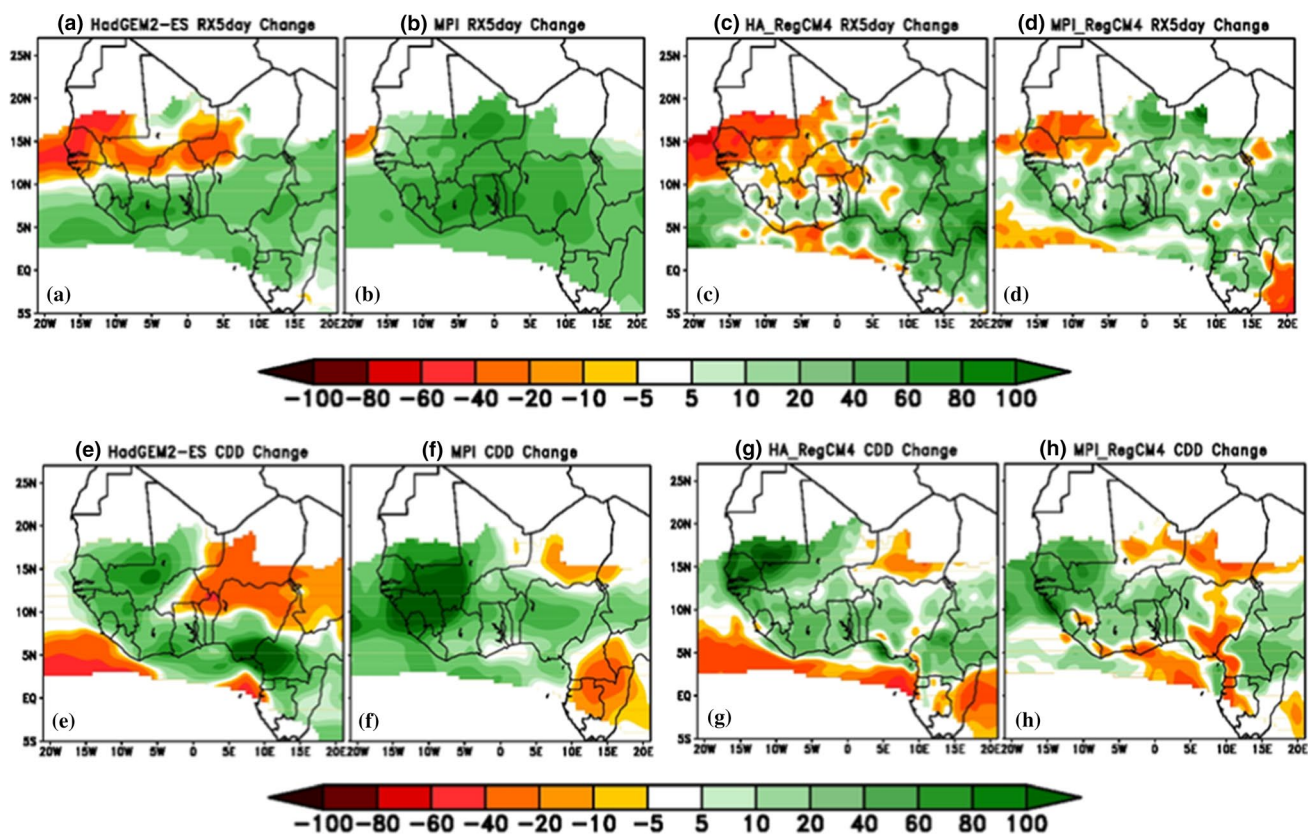
Fig. 10 Mean JJAS projected change [(2071–2100) minus (1976–2005)] in maximum five-day rainfall—RX5day (*top panels*; **a–d**) and maximum number of consecutive dry days (i.e. dry spells length)—CDD (*bottom panels*; **e–h**) from: HadGEM2-ES (**a**, **e**), MPI (**b**, **f**), HA_RegCM4 (**c**, **g**) and MPI_RegCM4 (**d**, **h**). The change is expressed in percent with respect to the 1976–2005 reference periods

especially in regions above 5°N, as this is where most of the evaporation decrease and precipitation increase occur. Generally, the ESMs exhibit a tendency towards simulating a moisture deficit over the highlands, implying a decrease in soil moisture which in turn is in agreement with the weakened evaporation (see Fig. 14a, b) due likely to less projected surface warming (not shown) around complex terrains.

To further investigate the regional features of the water budget component changes, we considered the three West African sub-domains of Fig. 1, which present different climatic regimes as shown in Fig. 4. Figure 15 displays time series of evaporation (Evap), precipitation (Precip) and its balance (Evap − Precip; i.e. E − P) changes based on the RCP 8.5 scenario for the Guinea, Sahel and West Africa (WA) regions over the period 2006–2100. HadGEM2-ES and MPI show mostly a positive trend in both precipitation and evaporation over all regions, in particular over Guinea and WA, with the change in E being smaller than that of P (i.e. E < P) and resulting in a deficit of local moisture supply. This localized moisture deficiency in both ESMs becomes more obvious from the early second half of the twenty-first century (~2060).

Precipitation changes in HA_RegCM4 show a negative trend over all regions whereas the evaporation shows a positive trend over Guinea. The difference E–P increases considerably, indicating an increase in freshwater deficit with HA_RegCM4 from the middle of the twenty-first century. On the other hand, there is not a clear trend of the precipitation change in MPI over the Sahel, but E–P changes show a discernible decrease trend over both Sahel and WA. Furthermore over the Sahel, in MPI_RegCM4 both evaporation and precipitation show negative trends, in agreement with the HA_RegCM4 projected pattern in this region. Our water budget analysis suggests that the Sahel, in particular the western Sahel, would likely undergo a slowing down of the hydrological cycle via a weakening of the water transport into the region (see discussion Fig. 12), which in turn inhibits precipitation and local moisture recycling.

Overall, we can conclude that the hydrological cycle over the WAM regions will be greatly affected by the global warming; nevertheless a large uncertainty still remains when comparing RegCM4 and the driving ESMs. However, the pattern of changes in water balance components over the Sahel is similar in both RegCM4 simulations (HA_RegCM4 and MPI_RegCM4), suggesting that the
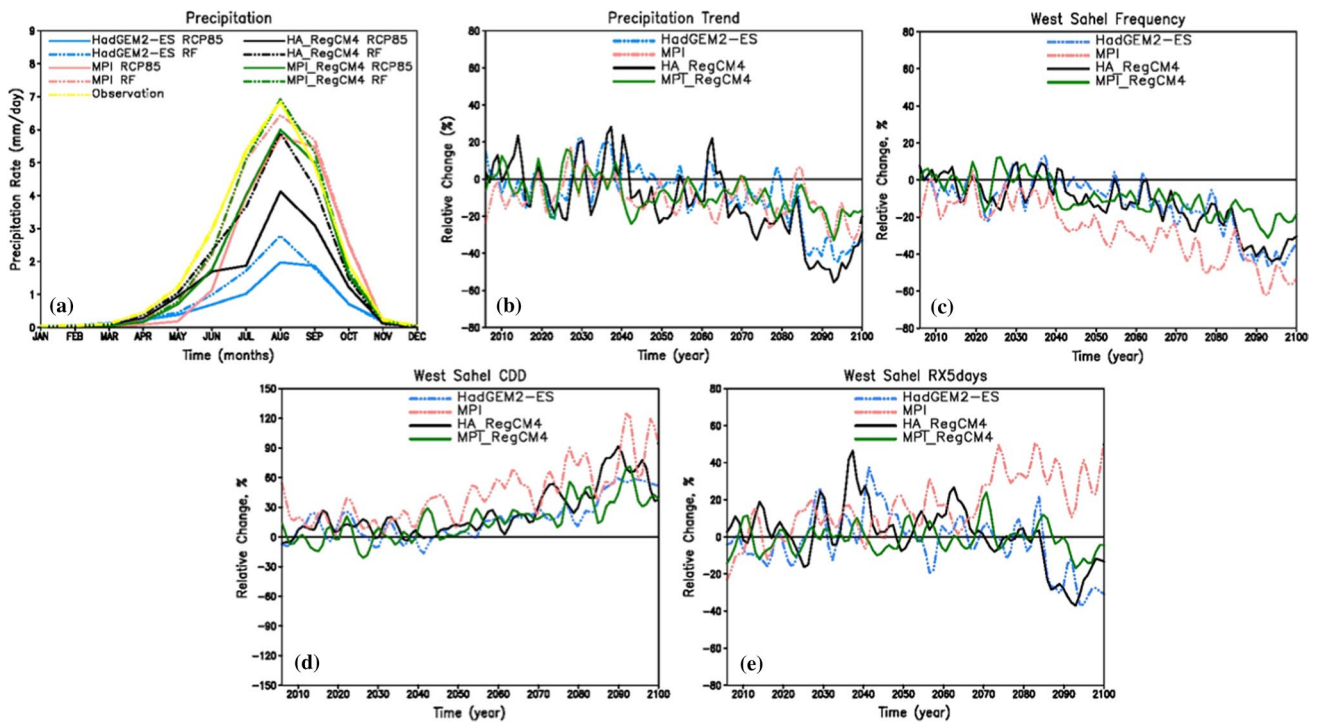
Fig. 11 Mean seasonal cycle over West Sahel for: **a** the reference period (*dashed line*, in mm) and the future (2071–2100 i.e. RCP 8.5; solid line; in mm/day). Trends of the changes over West Sahel for: **b** mean rainfall (expressed in %), **c** mean daily precipitation frequency, **d** maximum Consecutive dry days (CDD i.e. dry spells) and **e** maximum 5 day-intesity (RX5day). The changes in precipitation mean daily frequency, CDD, and RX5day are expressed in percent with respect to the 1976–2005 reference periods

hydrological cycle component in this region may probably be tied to local processes rather than large scale conditions.

The vertically integrated moisture flux (vectors) and divergence (shaded) in the bottom layer (1000–850 hPa), Fig. 16a–d) and upper layer (850–300 hPa), Fig. 16e–h) calculated from the ESMs, HA_RegCM4 and MPI_RegCM4 are shown in Fig. 16. The positive (negative) values represent convergence (divergence) in each grid box. For the bottom layer (1000–850 hPa), the ESMs and RegCM4 show an increase of the convergence area above 13°N, mostly eastward 10°W due to the strengthening of moisture flux originating from the Mediterranean Sea and the Congo basin (i.e. Central Africa). This is in line with the northward inland monsoon flux diverted toward east Sahel and discussed earlier (see Fig. 12). In fact, the precipitation increase over the east Sahel results in an enhancement of moisture convergence while the expected dryness over the west Sahel would likely be explained either by the simulated lower relative humidity (not shown) indicating a higher moisture deficit present in the late twenty-first century or to other dynamical processes in the upper levels (850–300 hPa).

In the upper level, the main convergence (divergence) areas are located below (above) 6°N in both AOGCMs and RegCM4, albeit a more pronounced and widespread divergence enhancement is projected around the Guinea highlands, Senegal and Mauritania in both HA_RegCM4 and MPI_RegCM4. Therefore, this mid-tropospheric divergence may be tied to the AEJ dynamics, known as an important channel of moisture transport over West Africa (e.g. Cook 1999; Abiodun et al. 2008; Nicholson 2013). In this respect, the ESMs and both RegCM4 experiments show an equatorward position and strengthening of the AEJ, in agreement to dry conditions over the western Sahel (e.g. Sylla et al. 2010; Diallo et al. 2013a, b). The equatorward position of the AEJ core coincides mostly with the divergence areas in the upper levels suggesting that the stronger AEJ divert the atmospheric moisture from the Sahel toward Atlantic Ocean. In summary, projected local (evaporation) and large scale processes (moisture convergence) change suggest that the rainfall increase over eastern and/or central Sahel would mainly be tied to elevated moisture convergence in the bottom layer (1000–850 hPa) due to increased water vapor in the bottom layer air column and surface evaporation. On the other hand, in the upper level (850–300 hPa), the strengthening of moisture divergence combined to both the southward migration of the AEJ as well as the weakening of rising motion between the core of AEJ and TEJ help to explain the projected dry condition over western Sahel.

Fig. 12 Mean JJAS projected change [(2071–2100) minus (1976–2005)] in mean sea level pressure (mslp; in *shaded* and expressed in hPa) superimposed to the 925 hPa low level winds (vectors; expressed in m/s) from: **a** HadGEM2-ES, **b** MPI, **c** HA_RegCM4 and **d** MPI_RegCM4
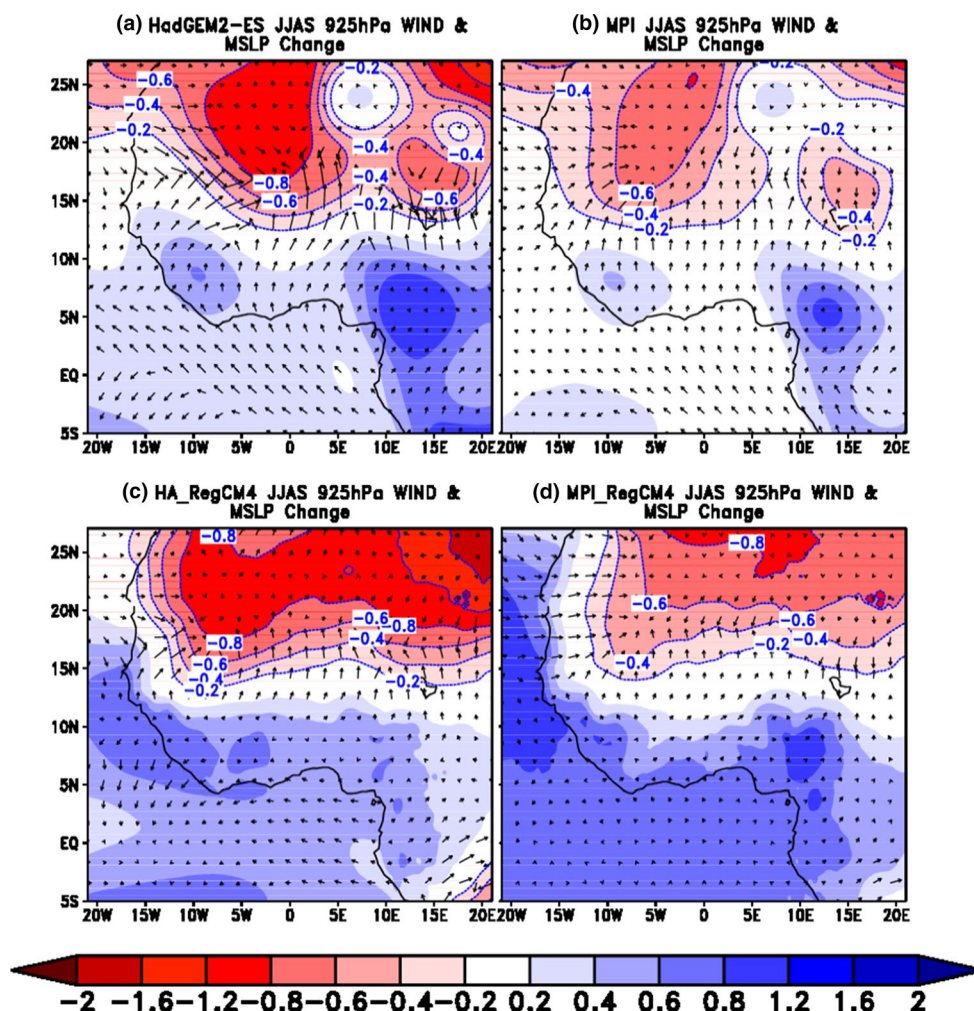
4 Summary and conclusions

In this study, we analyzed the CORDEX-Africa simulations carried out with RegCM4 to characterize not only changes in mean precipitation and its variability at different time-scale, but also on the projected changes in the hydrological cycle components and its impact on hydroclimatic regimes over West Africa during the peak of the West African Monsoon season (June–July–August–September; JJAS) for the late twenty-first century period (2071–2100). The model is run at a horizontal grid-spacing of 50 km over the whole Africa and is driven by two ESMs, the Earth system version of the Max-Planck-Institut für Meteorologie (MPI-ESM; MPI hereafter) and the Hadley Global Environmental 2—Earth System (HadGEM2-ES), for the period 1970–2100 under the RCP8.5 emission scenario. For the reference period (1976–2005), model mean precipitation, interannual variability and seasonal cycle are validated against different observational sources (CRU, UDEL, TRMM as well as GPCP), while large scale atmospheric circulations are compared to the pseudo-observed datasets from ERA-Interim

and NCEP/NCAR reanalysis. A number of selected precipitation extreme indices are validated against satellites-estimates from TRMM and GPCP.

Both RegCM4 (HA_RegCM4 and MPI_RegCM4) simulations realistically simulate the seasonal evolution of mean precipitation as well as the associated large scale circulation patterns for the current-climate, although some deficiencies (dry/wet biases) are evident. RegCM4 simulations improve the driving AOGCMs (HadGEM2-ES and MPI) features, especially the northward location of the ITCZ and the wet (dry) biases, due to an accurate representation of the temperature gradient between the Sahara and the Gulf of Guinea. Concerning the interannual variability and the extreme event indices, results show that, overall the ESMs compare better to the coarser resolution GPCP and the RegCM4 experiments are closer to the higher resolution TRMM, thus emphasizing the added value of the downscaling experiments.

In the late future, the mean precipitation is projected to decrease (increase) over western (central and/or eastern) Sahel, in agreement with recent studies using either
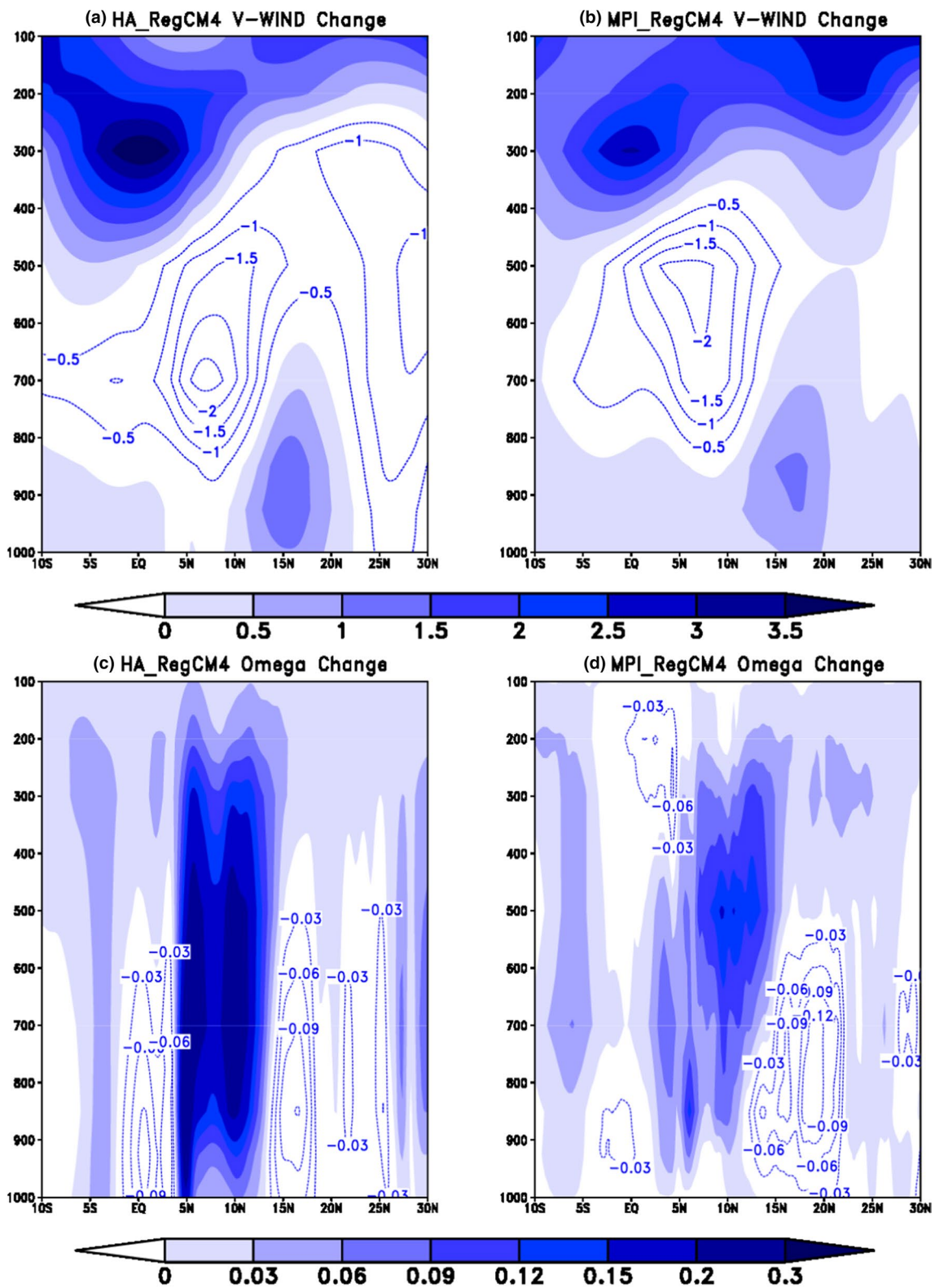
Fig. 13 Mean projected change [(2071–2100) minus (1976–2005)] in mean meridional wind—V-Wind (*top panels*; **a**, **b**; in m/s) and Omega (*bottom panels*; **c**, **d**; in 10^{-3} Pa/s) averaged over 10°W–10°E from: HA_RegCM4 (**a**, **c**) and MPI_RegCM4 (**b**, **d**)
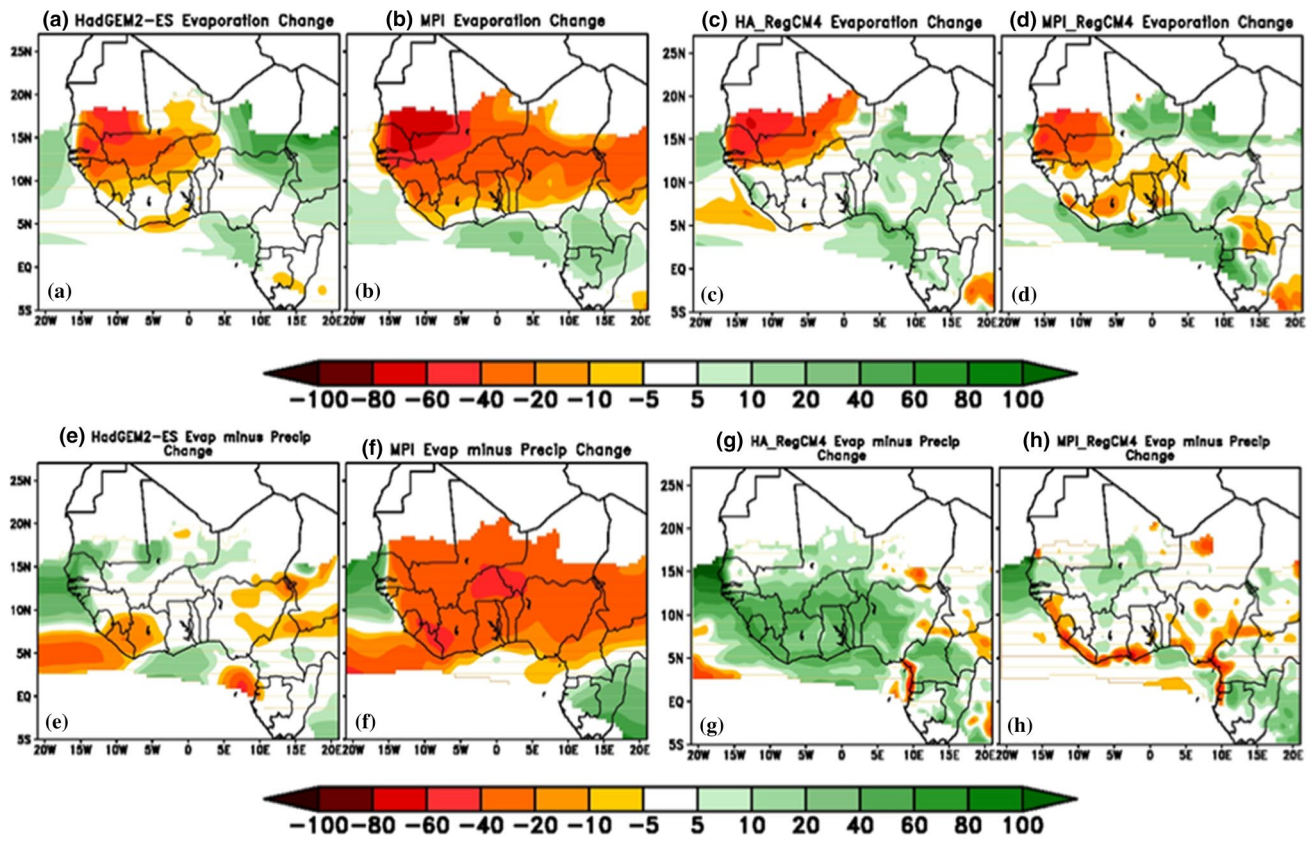
Fig. 14 Mean JJAS projected change [(2071–2100) minus (1976–2005)] in evaporation (*top panels*; **a–d**) and E–P (evaporation minus precipitation, *bottom panels*; **e–h**) from: HadGEM2-ES (**a**, **e**), MPI (**b**, **f**), HA_RegCM4 (**c**, **g**) and MPI_RegCM4 (**d**, **h**). The change is expressed in percent with respect to the 1976–2005 reference periods
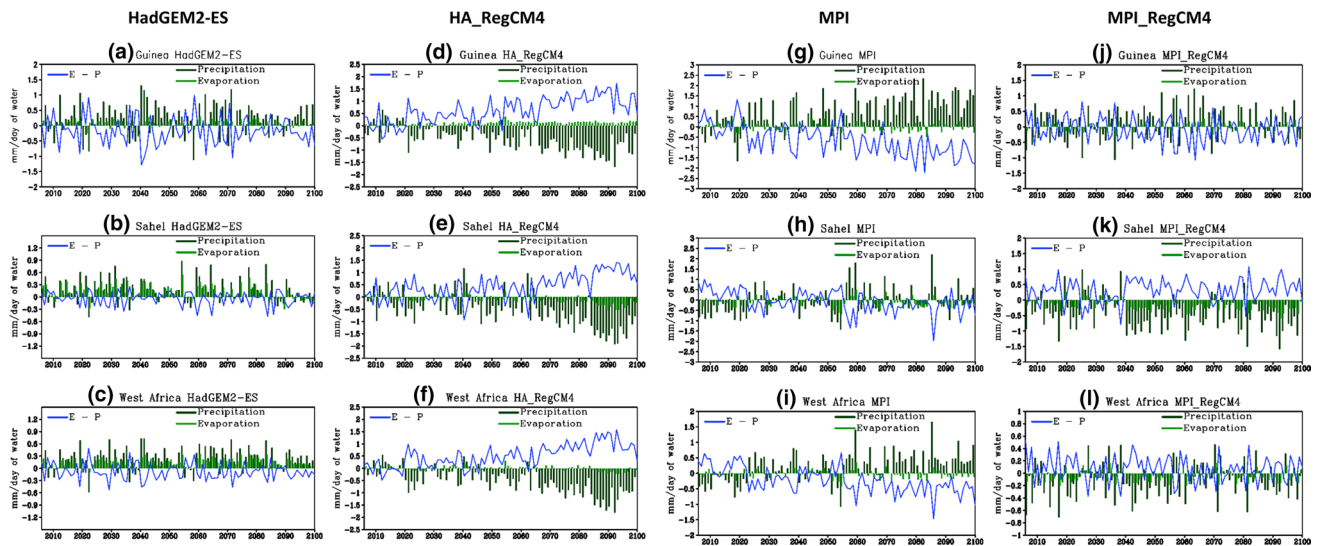
Fig. 15 Time series anomalies of the water budget components and its balance over the West African sub-domains [Guinea (*top panels*), Sahel (*middle panels*) and whole West Africa (*bottom panels*)] under RCP 8.5 projection scenario from RegCM4 and the two GCMs (HadGEM2-ES & MPI)
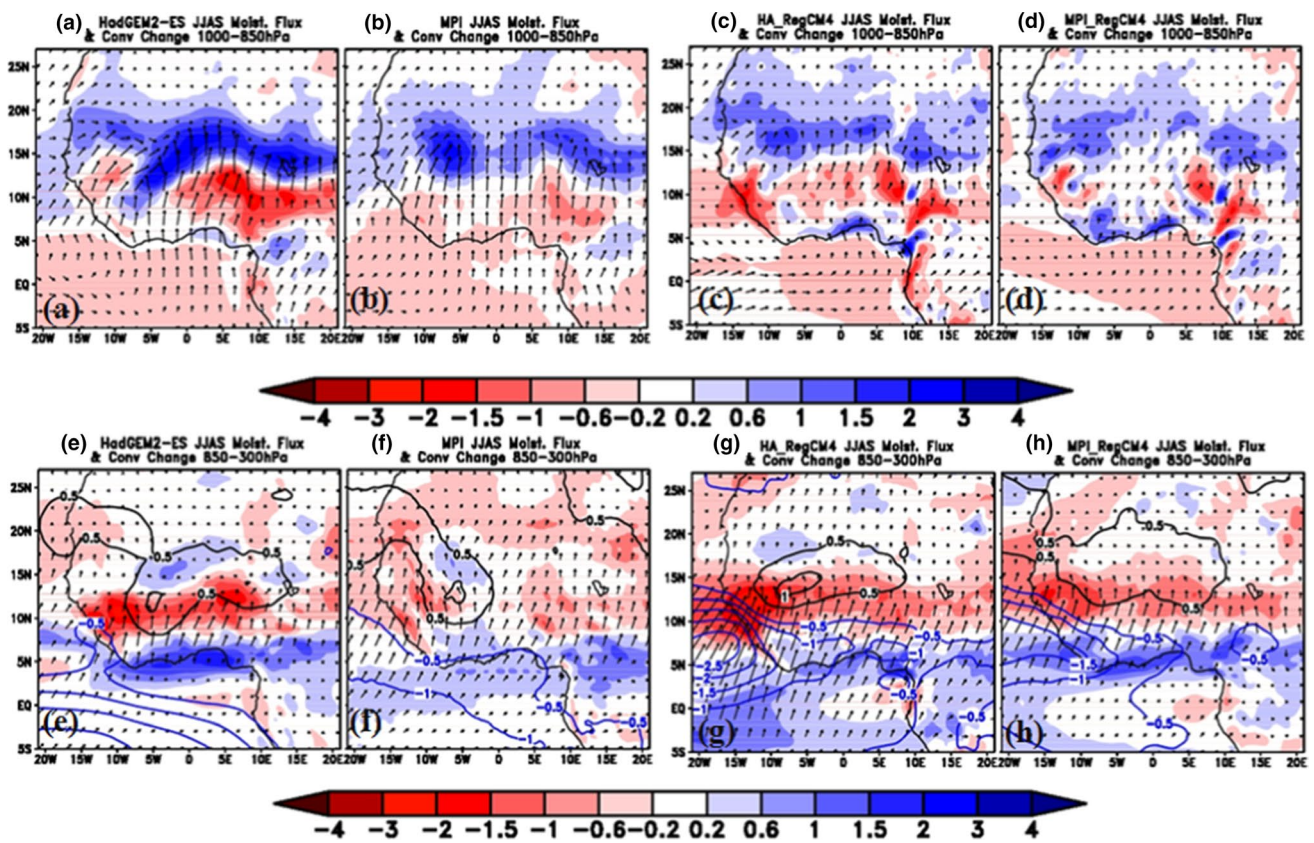
Fig. 16 Mean JJAS projected change [(2071–2100) minus (1976–2005)] in vertically integrated moisture flux Q (vectors, in kg. kg^{-1} × m.s^{-1}) and moisture divergence (shaded, × 10^{-4} s^{-1}) in bottom layer [(1000–850 hPa], *top panels*; **a–d**) and upper layer ([850–300 hPa], *bottom panels*; **e–h**) with in contours the 650 hPa zonal winds [m s^{-1}] from: HadGEM2-ES (**a, e**), MPI (**b, f**), HA_RegCM4 (**c, g**) and MPI_RegCM4 (**d, h**). *Blue contours* indicate a strengthening of the African Easterly Jet (AEJ) whereas *black contours* indicate a weakening of the AEJ. Here positive values (*blue color*) show convergence and negative values (*red color*) divergence

CORDEX simulations (e.g. Laprise et al. 2013; Mariotti et al. 2014) or CMIP5 data (e.g. Monerie et al. 2012). The pattern of change in R10mm and RX5day follow that of mean precipitation, emphasizing that the change in mean precipitation and extreme precipitation indices during the West African monsoon season are highly inter-related. The evaporation pattern change mainly follows that of mean precipitation in all models except MPI, thus suggesting that evaporation is not a major element contributing to precipitation change via recycling processes in MPI. Therefore, the change in both evaporation and precipitation will greatly affect the hydrological cycle. An analysis of the water balance component (Evaporation (E), Precipitation (P) and the budget E–P) over different sub-regions point out that over Sahel, the water balance components seem more likely tied to local processes rather than large scale conditions.

An analysis of vertically integrated moisture flux suggests that the rainfall increase over eastern and/or central Sahel would mainly be tied to moisture convergence contributed by the bottom layer (1000–850 hPa). Conversely the rainfall weakening over western Sahel results in an

increase in moisture divergence in the upper level (850–300 hPa) combined to both the southward migration of the AEJ as well as the weakening of rising motion located between above the core of AEJ and TEJ.

This study relies on a single regional climate model driven by two different AOGCMs for current and future climate. In order to provide more robustness to the climate change signal and its associated dynamical features, a multi-model ensemble is needed. We plan to compare our projection with other available one within the CORDEX-Africa program.

References

Abiodun BJ, Pal JS, Afiesimama EA, Gutowski WJ, Adedoyin A (2008) Simulation of West African monsoon using RegCM3 part II: impacts of deforestation and desertification. Theor Appl Climatol 93:245–261

Adler RF, Huffman GJ, Chang A, Ferraro R, Xie P, Janowiak J, Rudolf B, Schneider U, Curtis S, Bolvin D, Gruber A, Susskind J, Arkin P, Nelkin E (2003) The version-2 global precipitation climatology project (GPCP) monthly precipitation analysis (1979-present). J Hydrometeorol 4:1147–1167

Alpert P, Hemming D, Jin F, Kay G, Kitoh A, Mariotti A (2013) The hydrological cycle of the mediterranean. Adv Glob Change Res 50:201–239

Bhaskaran B, Ramachandran A, Jones R, Moufouma-Okia W (2012) Regional climate model applications on sub-regional scales over the Indian monsoon regions: the role of domain size on downscaling uncertainty. J Geophys Res 117:D10113. doi:10.1029/2012JD017956

Bouagila B, Sushama L (2013) On the current and future dry spell characteristics over Africa. Atmosphere 4(3):272–298

Chen TC, Yen MC, Murakami M (1988) The water vapor transport associated with the 30–50 day oscillation over the Asian monsoon regions during 1979 summer. Mon Weather Rev 116:1983–2002

Cook KH (1999) Generation of the African easterly jet and its role in determining West African precipitation. J Clim 12:1165–1184

Cook K, Vizy EK (2006) Coupled model simulations of the West African monsoon system: 20th and 21st century simulations. J Clim 19:3681–3703

Coppola E et al (2014) The bias and climate change signal in the Phase I CREMA experiment. Clim Change 125(1):23–38. doi:10.1007/s10584-014-1137-9

Dee et al (2011) The ERA-Interim reanalysis: configuration and performance of the data assimilation system. Quat J R Meteorol Soc 137:553–597. doi:10.1002/qj.828

Diallo I (2015) Caracterisation du cycle de l'eau dans le systéme de mousson de l'Afrique de l'Ouest et son évolution dans un contexte de changement climatique. Ph.D. Thesis, Cheikh Anta Diop University. Sénégal. 362 pp

Diallo I, Camara M, Sylla MB, Gaye AT (2010) Représentation haute résolution du systéme de mousson Ouest Africain avec un modéle climatique régional. Journal des Sciences Pour l'Ingénieur No 12:75–85. Disponible sur. http://www.ajol.info/index.php/jspi/article/viewFile/67978/56073

Diallo I, Sylla MB, Giorgi F, Gaye AT, Camara M (2012) Multi-model GCM-RCM ensemble based projections of temperature and precipitation over West Africa for the early twenty-first century. Int J Geophys. doi:10.1155/2012/972896

Diallo I, Sylla MB, Gaye AT, Camara M (2013a) Comparaison du climat et de la variabilité interannuelle de la pluie simulée au Sahel par les modèles climatiques régionaux. Sécheresse. doi:10.1684/sec.2013.0382

Diallo I, Sylla MB, Camara M, Gaye AT (2013b) Interannual variability of rainfall over the Sahel based on multiple regional climate models simulations. Theor Appl Climatol. doi:10.1007/s00704-012-0791-y

Diallo I, Bain CL, Gaye AT, Moufouma-Okia W, Niang C, Dieng MDB, Graham R (2014) Simulation of the Wes African monsoon onset using the HadGEM3-RA regional climate model. Clim Dyn 43(3–4):575–594. doi:10.1007/s00382-014-2219-0

Diallo I, Giorgi F, Sukumaran S, Stordal F, Giuliani G (2015) Evaluation of RegCM4 driven by CAM4 over Southern Africa: mean climatology, interannual variability and daily extremes of wet season temperature and precipitation. Theor Appl Climatol. doi:10.1007/s00704-014-1260-6

Dickinson RE, Henderson-Sellers A, Kennedy P (1993) Biosphere–atmosphere transfer scheme (BATS) version 1e as coupled to the NCAR community climate model. Tech Rep, National Center for Atmospheric Research Tech Note NCAR.TN-387+STR, NCAR, Boulder, CO

Druyan LM (2011) Studies of twenty-first century precipitation trends over West Africa. Int J Climatol 31:1415–1572. doi:10.1002/joc.2180

Druyan LM, Feng J, Cook K, Xue Y et al (2010) The WAMME regional model intercomparison study. Clim Dyn 35:175–192

Emanuel KA (1991) A scheme for representing cumulus convection in large-scale models. J Atmos Sci 48:2313–2335

Emanuel KA, Rothman MZ (1999) Development and evaluation of a convection scheme for use in climate models. J Atmos Sci 56:1756–1782

Gbobaniyi E, Sarr A, Sylla MB, Diallo I, Lennard C, Diedhiou A et al (2013) Climatology, annual cycle and interannual variability of precipitation and temperature in CORDEX regional climate models simulation over West Africa. Int J Climatol. doi:10.1002/joc.3834

Giorgi F (2002) Dependence of surface climate interannual variability on spatial scale. Geophys Res Lett 29:2101

Giorgi F, Jones C, Asrar GR (2009) Addressing climate information needs at the regional level: the CORDEX framework. WMO Bull 58:175–183

Giorgi F, Mearns LO (1999) Introduction to special section: regional climate modelling revisited. J Geophys Res 104:6335–6352

Giorgi F, Marinucci MR, Bates G (1993a) Development of a second generation regional climate model (RegCM2). I. Boundary layer and radiative transfer processes. Mon Weather Rev 121:2794–2813

Giorgi F, Marinucci MR, Bates G, DeCanio G (1993b) Development of a second generation regional climate model (RegCM2). II. Convective processes and assimilation of lateral boundary conditions. Mon Weather Rev 121:2814–2832

Giorgi F, Im ES, Coppola E, Diffenbaugh NS, Gao XJ, Mariotti L, Shi Y (2011) Higher hydroclimatic intensity with global warming. J Clim. doi:10.1175/2011JCLI3979.1

Giorgi F, Coppola E, Solmon F, Mariotti L, Sylla MB, Bi X, Elguindi N, Diro GT, Nair V, Giuliani G, Turuncoglu UU, Cozzini S, Güttler I, O'Brien TA, Tawfik AB, Shalaby A, Zakey AS, Steiner AL, Stordal F, Sloan LC, Brankovic C (2012) RegCM4: model description and preliminary tests over multiple CORDEX domains. Clim Res 52:7–29. doi:10.3354/cr01018

Giorgi F and Coauthors (2014) Changes in extremes and hydroclimatic regimes in the CREMA ensemble projections. Clim Change. doi:10.1007/s10584-014-1117-0

Grell G, Dudhia J, Stauffer DR (1994) A description of the fifth generation Penn State/NCAR Mesoscale Model (MM5). National Center for Atmospheric Research Tech Note NCAR/TN-398+STR, NCAR, Boulder, CO

Harris I, Jones PD, Osborn TJ, Lister DH (2013) Updated high-resolution grids of monthly climatic observations. Int J Climatol. doi:10.1002/joc.3711

Hernández-Díaz L, Laprise R, Sushama L, Martynov A, Winger K, Dugas B (2012) Climate simulation over the CORDEX-Africa domain using the fifth generation Canadian Regional Climate Model (CRCM5). Clim Dyn. doi:10.1007/s00382-012-1387-z

Holtslag A, de Bruijn E, Pan HL (1990) A high resolution air mass transformation model for short-range weather forecasting. Mon Weather Rev 118:1561–1575

Huffman GJ, Adler RF, Bolvin DT, Gu G, Nelkin EJ, Bowman KP, Hong Y, Stocker EF, Wolff DB (2007) The TRMM multisatellite precipitation analysis: quasi-global, multi-year, combined-sensor precipitation estimates at fine scale. J Hydrometeorol 8:38–55

Huffman GJ, Adler RF, Bolvin DT, Gu G (2009) Improving the global precipitation record: GPCP Version 2.1. Geophys Res Lett. doi:10.1029/2009GL040000

IPCC (2007) Summary for policymakers. In: Solomon S, Qin D, Manning M, Chen Z, Marquis M, Averyt KB, Tignor M, Miller HL (eds) Climate change 2007: the physical science basis contribution of working group I to the fourth assessment report (AR4) of the intergovernmental panel on climate change. Cambridge University Press, Cambridge

IPCC (2008) Towards new scenarios for analysis of emissions, climate change impacts and response strategies. IPCC Expert Meeting Report onNew Scenarios, Noordwijkerhout, Intergovernmental Panel on Climate Change

Jones C, Giorgi F, Asrar G (2011) The coordinated regional downscaling experiment (CORDEX). An international downscaling link to CMIP5. Cliv Exch 16:34–40

Kanamitsu M, Ebisuzaki W, Woollen J et al (2002) NCEPDOE AMIP-II reanalysis (R-2). Bull Am Meteorol Soc 83(11):1631–1643

Kiehl J, Hack J, Bonan G, Boville B, Breigleb B, Williamson D, Rasch P (1996) Description of the NCAR Community Climate Model (CCM3). National Center for Atmospheric Research Tech Note NCAR/TN-420 + STR, NCAR, Boulder, CO

Klutse NA, Sylla MB, Diallo I, Sarr A, Dosio A, Diedhiou A, Kamga A, Lamptey B, Ali A, Gbobaniyi EO, Owusu K et al (2016) Daily characteristics of West African summer monsoon precipitation in CORDEX simulations. Theor Appl Climatol 123(1):369–386. doi:10.1007/s00704-014-1352-3

Laprise R, Hernàndez-Diaz Tete K, Sushama L, Separovic L, Martynov A, Winger K, Valin M (2013) Climate projections over CORDEX Africa domain using the fifth-generation. Can Reg Clim Model (CRCM5). doi:10.1007/s00382-012-1651-2

Legates DR, Willmott CJ (1990) Mean seasonal and spatial variability in gauge-corrected, global precipitation. Int J Climatol 10:111–127

Li L, Diallo I, Xu CY, Stordal F (2015) Hydrological projections under climate change in the near future by RegCM4 in Southern Africa using a large-scale hydrological model. J Hydrol 528:1–16

Mariotti A (2010) Recent changes in mediterranean water cycle: a pathway toward long-term regional hydroclimatic change? J Clim 23:1513–1525

Mariotti A, Zeng N, Yoon JH, Artale V, Navarra A, Alpert P, Li ZX (2008) Mediterranean water cycle changes: transition to drier twenty-first century conditions in observations and CMIP3 simulations. Environ Res Lett. doi:10.1088/1748-9326/3/4/044001

Mariotti L, Coppola E, Sylla MB, Giorgi F, Piani C (2011) Regional climate model simulation of projected twenty-first century climate change over an all-Africa domain: comparison analysis of nested and driving model results. J Geophys Res 116:D15111. doi:10.1029/2010JD015068

Mariotti L, Diallo I, Coppola E, Giorgi F (2014) Seasonal and intraseasonal changes of African monsoon climates in twenty-first century CORDEX projections. Clim Change. doi:10.007/s10584-014-1097-0

Monerie PA, Fontaine B, Roucou P (2012) Expected future changes in the African monsoon between 2030 and 2070 using some CMIP3 and CMIP5 models under a medium-low RCP scenario. J Geophys Res 117:D16111. doi:10.1029/2012JD017510

Moufouma-Okia W, Jones R (2015) Resolution dependence in simulating the African hydroclimate with the HadGEM3-RA regional climate model. Clim Dyn 44(3–4):609–632

Music B, Caya D (2009) Investigation of the sensitivity of water cycle components simulated by the Canadian Regional Climate Model to the land surface parameterization, the lateral boundary data, and the internal variability. J Hydrometeorol 10(1):3–21

Nicholson SE (2009) A revised picture of the structure of the "monsoon" and land ITCZ over West Africa. Clim Dyn 32:1155–1171. doi:10.1007/s00382-008-0514-3

Nicholson SE (2013) The West Sahel: a review of recent studies on the rainfall regime and its interannual variability. Meteorology. doi:10.1155/2013/453521

Nikulin G, Jones C, Samuelsson P, Giorgi F, Asrar G, Büchner M, Cerezo-Mota R, Christensen OB, Déqué M, Fernandez J, Hänsler A, van Meijgaard E, Sylla MB, Sushama L (2012) Precipitation climatology in an ensemble of CORDEX-Africa Regional Climate simulations. J Clim. doi:10.1175/JCLI-D-11-00375.1

Oettli P et al (2011) Are regional climate models relevant for crop yield prediction in West Africa? Environ Res Lett 6(1):014008

Oki T, Musiake K, Matsuyama H, Masuda K (1995) Global atmospheric water balance and runoff from large river basins. Hydrol Process 9:655–678

Oleson K, Niu GY, Yang ZL, Lawrence DM, Thornton PE, Lawrence PJ, Stöckli R, Dickinson RE, Bonan GB, Levis S, Dai A, Qian T (2008) Improvements to the community land model and their impact on the hydrological cycle. J Geophys Res. doi:10.1029/2007JG000563

Otieno VO, Anyah RO (2013) CMIP5 simulated climate conditions of the Greater Horn of Africa (GHA). Part II: projected climate. Clim Dyn. doi:10.1007/s00382-013-1694-z

Paeth H, Hall NMJ, Gaertner MA, Alonso MD, Moumouni S, Polcher J, Ruti PM, Fink AH, Gosset M, Lebel T, Gaye AT, Rowell DP, Moufouma-Okia W, Jacob D, Rockel B, Giorgi F, Rummukainen M (2011) Progress in regional downscaling of West African precipitation. Atmos Sci Lett 12:75–82. doi:10.1002/asl.306

Pal JS, Small E, Eltahir E (2000) Simulation of regional-scale water and energy budgets: representation of subgrid cloud and precipitation processes within RegCM. J Geophys Res 105:29579–29594

Pal and Coauthors (2007) Regional climate modeling for the developing world: the ICTP RegCM3 and RegCNET. Bull Amer Meteor Soc 88:1395–1409

Panitz HJ, Dosio A, Büchner M, Lüthi D, Keuler K (2013) COSMO-CLM (CCLM) climate simulations over CORDEX-Africa domain: analysis of the ERA-interim driven simulations at 0.44° and 0.22° resolution. Clim Dyn. doi:10.1007/s00382-013-1834-5

Peixoto JP, Oort AH (1992) Physics of climate. American Institute of Physic, New York, 520

Prasanna V, Yasunari T (2011) Simulated changes in the atmospheric water balance over South Asia in the eight IPCC AR4 coupled climate models. Theor Appl Climatol 104(1–2):139–158

Rummukainen M (2010) State-of-the-art with regional climate models. Clim Change 1:82–96

Ruti PM et al (2011) The West African climate system: a review of the AMMA model inter-comparison initiatives. Atmos Sci Lett 12:116–122

Saeed F, Haensler A, Weber T, Hangemann S, Jacob D (2013) Representation of extreme precipitation events leading to opposite climate change signals over the Congo Basin. Atmosphere 4:254–271. doi:10.3390/atmos4030254

Seneviratne SI, Viterbo P, Luthi D, Schar C (2004) Inferring changes in terrestrial water storage using ERA-40 reanalysis data: the Mississippi River Basin. J Clim 17:2039–2057

Seth A, Rauscher SA, Biasutti M, Giannini A, Camargo S, Rojas M (2013) CMIP5 Projected changes in the annual cycle of precipitation in monsoon regions. J Clim. doi:10.1175/JCLI-D-12-00726.1

Siam MS, Demory ME, Eltahir EAB (2013) Hydrological cycle over the Congo and Upper Blue Nile Basins: evaluation of general circulation model simulations and reanalysis products. J Clim 26:8881–8894. doi:10.1175/JCLI-D-12-00404.1

Sillmann J, Kharin VV, Zhang X, Zwiers FW, Bronaugh D (2013a) Climate extreme indices in the CMIP5 multimodel ensemble: part 1. Model evaluation in the present climate. J Geophys Res Atmos 118:1716–1733. doi:10.1002/jgrd.50203

Sillmann J, Kharin VV, Zwiers FW, Zhang X, Bronaugh D (2013b) Climate extreme indices in the CMIP5 multimodel ensemble: part 2. Future climate projections. J Geophys Res Atmos 118:2473–2493. doi:10.1002/jgrd.50188

Steiner A, Pal JS, Rauscher S, Bell J, Diffenbaugh N, Boone A, Sloan L, Giorgi F (2009) Land surface coupling in regional climate simulations of the West African monsoon. Clim Dyn 33:869–892

Sylla MB, Gaye AT, Jenkins GS, Pal JS, Giorgi F (2010) Consistency of projected drought over the Sahel with changes in the monsoon circulation and extremes in a regional climate model projections. J Geophys Res 115:D16108. doi:10.1029/2009JD012983

Sylla MB, Gaye AT, Jenkins GS (2012) On the fine-scale topography regulating changes in atmospheric hydrological cycle and extreme rainfall over west africa in a regional climate model projections. Int J Geophys. doi:10.1155/2012/981649

Sylla MB, Diallo I, Pal JS (2013a) West African monsoon in state-of-the-science regional climate models. Climate Variability: Regional and Thematic Patterns, A. Tarhule, (Ed) ISBN: 978-953-51-1187-0, InTech, 3–36. doi:10.5772/55140. Available from http://www.intechopen.com/books/climate-variability-regional-and-thematicpatterns/west-african-monsoon-in-state-of-the-science-regional-climate-models

Sylla MB, Giogi F, Coppola E, Mariotti L (2013b) Uncertainties in daily rainfall over Africa: assessment of gridded observation products and evaluation of a regional climate model simulation. Int J Climatol. doi:10.1002/joc.3551

Tebaldi C, Hayhoe K, Arblaster JM, Meehl GA (2006) Going to the extremes. An intercomparison of model-simulated historical and future changes in extreme events. Clim Change 79:185–211. doi:10.1007/s10584-006-9051-4

Trenberth KE (1999) Atmospheric moisture recycling: role of advection and local evaporation. J Clim 12:1368–1381

Trenberth KE (2011) Changes in precipitation with climate change. Clim Res 47:123–138. doi:10.3354/cr00953

Van Den Hurk BJJM, Van Meijgaard E (2010) Diagnosing land-atmosphere interaction from a regional climate model simulation over West Africa. J Clim. doi:10.1175/2009JHM1173.1

Van der Linden P, Mitchell JFB (2009) ENSEMBLES: climate change and its impact: summary of research and the results from the ENSEMBLES project. Met Office Hadley Centre, Exeter, p 160

Vellinga M, Arribas A, Graham R (2013) Seasonal forecasts for regional onset of the West African monsoon. Clim Dyn. doi:10.1007/s00382-012-1520-z

Vizy E, Cook K, Crétat J, Neupane N (2013) Projections of a Wetter Sahel in the twenty-first Century from global and regional models. J Clim. doi:10.1175/JCLI-D-12-00533.1

Xue Y, De Sales F, Lau KMW, Bonne A, Feng J, Dirmeyer P, Guo Z, Kim KM, Kitoh A, Kumar V, Poccard-Leclercq I, Mahowald N, Moufouma-Okia W, Pegion P, Rowell DP, Schemm J, Schubert S, Sealy A, Thiaw WM, Vintzileos A, Williams SF, Wu ML (2010) Intercomparison of West African Monsoon and its variability in the West African Monsoon Modelling Evaluation Project (WAMME) first model Intercomparison experiment. Clim Dyn 35:3–27. doi:10.1007/s00382-010-0778-2

Zaroug MAH, Sylla MB, Giorgi F, Eltahir EAB, Aggarwal PK (2013) A sensitivity study on the role of the swamps of southern Sudan in the summer climate of North Africa using a regional climate model. Theor Appl Climatol 113:63–81. doi:10.1007/s00704-012-0751-6

Zeng X, Zhao M, Dickinson RE (1998) Intercomparison of bulk aerodynamic algorithms for the computation of sea surface fluxes using TOGA COARE and TAO data. J Clim 11:2628–2644